공학석사 학위논문

Nano-carbonate hydroxyapatite synthesis through CO_2 absorption and wet precipitation

이산화탄소 포집과 침전법을 이용한 나노 탄산 하이드록시아파타이트의 합성

2016년 2월

서울대학교 대학원

재료공학부

이 혜 경

Abstract

Nano-carbonate hydroxyapatite synthesis through CO_2 absorption and wet precipitation

Hye Kyoung Lee

Department of Materials Science and Engineering

The Graduate School

Seoul National University

Calcium phosphate compounds are used as a bone implant material for the treatment of bond related disease or injury. Among many calcium phosphate compounds, hydroxyapatite (HAP, $Ca_{10}(PO_4)_6(OH)_2$) and β-tricalcium phosphate (β-TCP, $Ca_3(PO_4)_2$) are the most widely used. Although the major components of natural bone are calcium and phosphate, there are many other ions in the bone such as carbonate, sodium, and kalium. Therefore, many studies about ion substitution in HAP were reported. Especially, the carbonate substituted hydroxyapatite is of great interest because of its composition similarity with natural bone and potential to enhance bioactivity of bone grafts. There are many carbonate hydroxyapatite synthesis methods, but most of them use carbon containing chemical for the source of substituted carbonate during the synthesis.

In this research, nano-carbonate hydroxyapatite (CHA) was successfully synthesized through wet precipitation method in aqueous solution. By creating superoxide anion radical in the system, atmospheric CO_2 was captured and used as a source of carbonate groups in CHA. CHA formation

was confirmed using XRD and FT-IR analysis, and comparison study between synthesized CHA and HAP was carried out. The gas chromatography result showed that our CHA synthesis system absorbed large amount of CO_2 in the air efficiently. After that, we observed phase transformation occurred during the CHA synthesis. The result showed that dicalcium phosphate dehydrate (DCPD) was intermediate phase of CHA. Lastly, we succeeded in controlling substituted CO_3 amount in CHA by controlling used H_2O_2 amount. As a result, we successfully synthesized CHA with bone similar composition.

This research has two major impacts. First of all, this synthesis method proposes a new way to mineralize large amount of atmospheric CO_2 and use the mineralized form of CO_2 as the carbon source of CHA. Second, synthesized CHA can be used as bone implant material because of its chemical composition similarity to natural bone. Consequently, our CHA synthesis system presents the innovative method for synthesizing bone implant material while capturing atmospheric CO_2.

Keywords: carbonate hydroxyapatite, wet precipitation, CO_2 absorption, superoxide anion radical, implant material, bone

Student Number: 2014-21458

CONTENTS

List of Tables

List of Figures

Chapter 1. INTRODUCTION

1.1 Introduction of biominerals and calcium phosphate compounds as bond implant material

Living organisms in nature can make inorganic compounds through the interactions with surrounding ecological environment[1]. These inorganic compounds can be defined as biominerals. Humans also have mineralized tissues inside their body, teeth and bone. Teeth brake down the food before entering the digestive system, and this make easy for the digestive organs to absorb nutrients in the food. Bone supports our body as the framework and protects the body's internal organs from the external shock. Additionally bone stores several minerals and produces produce blood cells. In this regard, hard tissues are considered as very important organs in the body.

1.1.1 Chemical composition of human bone

Bone is a heterogeneous composite material consisting a mineral phase, an organic phase, and water[2]. Of its dry mass, approximately 70% of mineral comprise of the bone[1]. Organic materials in human bone are known to be collagen, non-collagen proteins, and lipids[3]. Main components of mineral part of bone are Ca, P, CO_3, Na, and Mg, and their amount ranges are shown

Table 1.1 Main components' composition range in bone mineral[1,4]

Component	Range (wt%)
Ca	32.6 ~ 39.5
P	13.1 ~ 18.0
CO_3	2.3 ~ 8.0
Na	0.26 ~ 0.82
Mg	0.32 ~ 0.78
Citrate	0.04 ~ 2.67

in Table 1.1[1,4]. As shown in Table 1.1, calcium and phosphate take up large parts of the bone. In this regard, it is known that calcium phosphate compounds compose most inorganic parts of human bone[5,6]. Hydroxyapatite (HAP: $Ca_{10}(PO_4)_6(OH)_2$) is the primary calcium phosphate phase in the bone[1]. Therefore, calcium phosphate compounds such as synthetic HAP and β-tricalcium phosphate used as a bone graft material for bone disease treatments.

1.1.2 Requirements for bone implant material

For the efficient bone implant, the material has to provide suitable environment for bone regeneration. In this regard, a few requirements should be considered in the selection of bone graft material. First, the material should have biocompatibility[7]. This means that implanted material is neither toxic nor

carcinogenic to prevent the death of surrounding tissue. Second, the material should be biodegradable[7]. Because the ultimate goal of the treatment that using implant is allowing regenerated bone tissue to replace the grafted construct, the material used in bone implant should dissolve in the body without causing any problem. Finally, bioactivity is required for the bone graft material[8]. Bioactivity contains the meaning of osteoinductivity and osteointegrativity. Osteoinductivity is a property that makes stem cells differentiate into bone regenerating cells, and osteointegrativity is a property that allows the implant to connect with native bone by forming interfacial bone[8]. These properties promote bone regeneration and make implant act as native bone.

1.1.3 Synthetic calcium phosphate compounds as bone implant material: hydroxyapatite and β-tricalcium phosphate

According to the requirements for good bone implant material, synthetic HAP seems to be a proper material for bone substitution. Many studies reported that synthetic HAP has excellent biocompatibility and bioactivity[9-12]. It is observed that both osteoblasts and bone marrow cells which are the essential cells for bone regeneration adhered very well on the surface of synthetic HAP implants[9,10]. In addition, density of osteoblast and number of bone marrow cell was increased after seeding those cells on the HAP[9,10]. These results indicate that synthetic HAP is biocompatible. To verify

the bioactivity of synthetic HAP, stem cell differentiation and in vivo test was conducted[10-12]. According to previous research, alkaline phosphatase (ALP), an early biochemical marker for osteoblast differentiation, was expressed after seeding stem cells on the synthetic HAP surface[10,11]. Moreover, proteins namely ALP, type 1 collagen (COL1), and osteocalcin (OC) were highly expressed on the HAP, indicating the ability of synthetic HAP to induce osteoblast cells towards the maturation stage[9]. In the *in vivo* test, active bone formation and bone marrow formation between the HAP and native bone were observed, which demonstrating osteointegrativity of synthetic HAP[12]. Although synthetic HAP has been widely used as bone substitute because of its great biocompatibility and bioactivity, there are some limitations. The biggest problem is its high crystalline phase. Because of this high crystallinity, synthetic HAP hardly dissolves after the implantation[13]. Therefore, HAP cannot be replaced by newly formed bone, and remains for very long periods[14]. As a result, fracture may occur either in the HAP itself or at the interface with native bone, and this can cause serious deformity of the bone[14, 15].

To prevent the problem caused by remaining implant, biodegradable calcium phosphates have been developed. β-tricalcium phosphate (β-TCP) is one of the most widely used biodegradable bone graft material. It is also known to be biocompatible and osteoconductive like HAP[16-18]. However, β-TCP can be dissolved and replaced by newly formed bone because of its degradability while HAP was left for a long time after the surgery[14, 19]. Comparison of degradability of HAP and β-TCP after the implantation is

shown in Figure 1.1. Although β-TCP seems an ideal biomaterial for bone substitution, it also has limitation. The limitation is that β-TCP is not an actual biomineral in the body. β-TCP cannot be synthesized in the body because β-TCP is synthesized in the very high temperature condition[20]. Therefore, the heat treatment is required during the synthesis process. Considering this synthesis condition, it is virtually impossible that β-TCP is produced in the human body.

As aforementioned, synthetic HAP and β-TCP are well-known synthetic calcium phosphates for bone graft materials. The compositions of these inorganic compounds are calcium and phosphate groups. However, there are various ions in natural bone as shown in Table 1.1. Therefore, these synthetic calcium phosphate compounds cannot be same with natural bone because of its chemical composition difference. Therefore, many studies tried to substitute others ion in HAP structure to mimic natural bone.

Figure 1.1 Radiographs of a simple bone after the hydroxyapatite (HAP) and β-tricalcium phosphate (β-TCP) implantations[14]. The bright colored area in the bone indicates the bone implant materials. **a,** Grafted synthetic HAP implant remained in the body even after the 111 months after the implantation. **b,** At the first time, β-TCP was detected by radiographs, but gradually disappeared after the implantation.

1.2 Carbonate hydroxyapatite

As shown in Table 1.1, the detected amount of carbonate (CO_3) in natural bone is 2.3~8 wt %. As the table demonstrated, CO_3 is the third most abundant inorganic composition in the bone. Therefore, many studies tried to make CO_3 substituted hydroxyapatite (carbonate hydroxyapatite) that mimics chemical composition of actual bone for bone implant ceramic.

1.2.1 Types of carbonate hydroxyapatite

Substitution of CO_3 can occur in two different atomic sites in the hydroxyapatite[4]. Those two substituted sites are shown in Figure 1.2. First, hydroxyl ions (OH) in the HAP lattice can be substituted by CO_3, and this type of carbonate hydroxyapatite is termed A-type[21]. This type of carbonate hydroxyapatite can be synthesized by exchanging the OH ions in the stoichiometric HAP for CO_3 groups[22-24]. Well-known A-type carbonate hydroxyapatite synthesis method is exposing the stoichiometric HAP to the CO_2 abundant environment[23-25]. The very simple substitution mechanism of A-type is shown in following equation.

$$Ca_{10}(PO_4)_6(OH)_2 + xCO_2 \rightarrow Ca_{10}(PO_4)_6(OH)_{2-2x}(CO_3)_x + xH_2O$$

However, these synthesis methods are not very suitable for the biomedical

materials production. The methods exposing the stoichiometric HAP to the CO_2 abundant condition usually take very long reaction time, and carbonate substitution cannot be readily controlled. Because most of the CO_3 substitution will occur at the surface of the HAP, it is difficult to control carbonate substitution in all parts of the material. In addition, the mineral phase of bone is not solely A-type. Therefore, A-type carbonate hydroxyapatite is not appropriate for the direct bone replacement material.

The second type of carbonate hydroxyapatite is B-type carbonate hydroxyapatite. This type of carbonate hydroxyapatite is defined by the CO_3 ion substitution for phosphate ions in the hydroxyapatite lattice[4]. Generally, B-type carbonate hydroxyapatite was synthesized through the controlled precipitation method of carbonate apatite using calcium, phosphate, and carbonate containing reagent[26-28]. The B-type carbonate hydroxyapatite formula can be written in following form[1].

$$Ca_{10-2x/3}[(PO_4)_{6-x}(CO_3)_x](OH)_{2-x/3}$$

Because the charge of CO_3 ion and PO_4 ion is different, the formula is more complicated than the A-type carbonate hydroxyapatite. If a carbonate ion substitutes a phosphate, calcium and hydroxyl ions also should be changed to maintain charge balance. This charge difference problem also can be solved by using sodium ions. The B-type carbonated hydroxyapatite which containing sodium ion can be expressed in following formula[4].

$$Ca_{10-x}Na_x(PO_4)_{6-x}(CO_3)_x(OH)_2$$

Though this synthesis method has the problems in synthesizing pure B-type carbonate hydroxyapatite, this precipitation method is widely used for fabricating B-type carbonate hydroxyapatite. The two kinds of CO_3 substitution mentioned before can occur simultaneously, and mixed AB-type carbonate hydroxyapatite can be synthesized[29]. In addition, the calcium phosphate apatite that constitutes bone mineral is considered a mixed AB-type substitution[30].

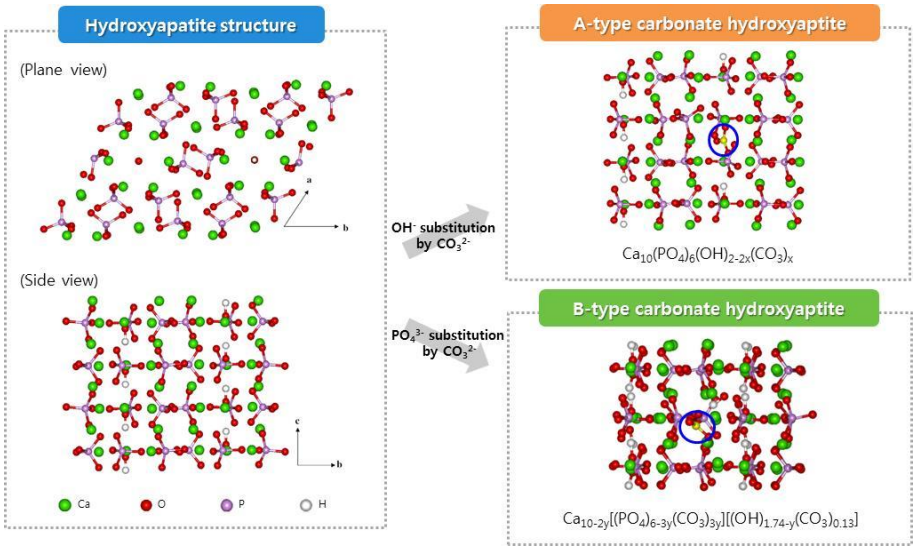

Figure 1.2 Two types of carbonate hydroxyapatite and two distinct atomic sites in hydroxyapatite.

1.2.2 Carbonate hydroxyapatite as bone implant material

These carbonate containing hydroxyapatite has gained much attention because of its functional properties for good bone graft material including similar chemical composition. Many studies reported that carbonate substituted hydroxyapatite is more soluble than hydroxyapatite[31,32]. Studies have demonstrated that substituted carbonate ion affect the crystallinity of hydroxyapatite, and caused lower the crystallinity and higher number of defect in the hydroxyapatite structure[33]. Because of this decreased crystallinity, the carbonate hydroxyapatite can have solubility after the implant. Another advantage of carbonate hydroxyapatite is its good biocompatibility and bioactivity. Osteoblasts were well attached and produced extracellular matrix on the carbonate hydroxyapatite surface[34]. The osteoblast on the CHA showed better collagen synthesis behavior than HAP[35]. As shown in Figure 1.3, the cell proliferation on the carbonate hydroxyapatite showed no significant difference compared to hydroxyapatite[34]. In addition, it was reported that activity of osteoclast and osteoblast was high on the carbonate substituted hydroxyapatite[35,36]. The comparison study of osteoclast and osteoblast activity on different substrates was shown in Figure 1.4. Moreover, carbonate hydroxyapatite showed good abilities in *in vivo* test. It showed higher osteoconductive properties and greater new bone formation compared to hydroxyapatite[37]. In conclusion, carbonate hydroxyapatite is similar to natural bone, and it has good biocompatibility and bioactivity. In addition, it is more

soluble compared to HAP, so it can be substituted by newly formed bone. Therefore, carbonate hydroxyapatite could be better bone implant material than HAP.

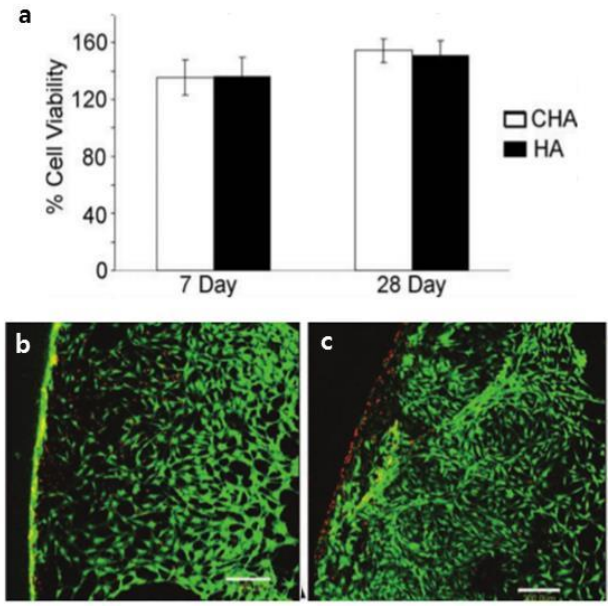

Figure 1.3 Comparison study of biocompatibility between carbonate hydroxyapatite (CHA) and hydroxyapatite (HAP). **a,** cell viability on the CHA and HA. **b-c,** Images of live/dead staining of cells on **b,** CHA disc. **c,** HA disc (culturing day: 21 days). Scale bar = 200μm.[34]

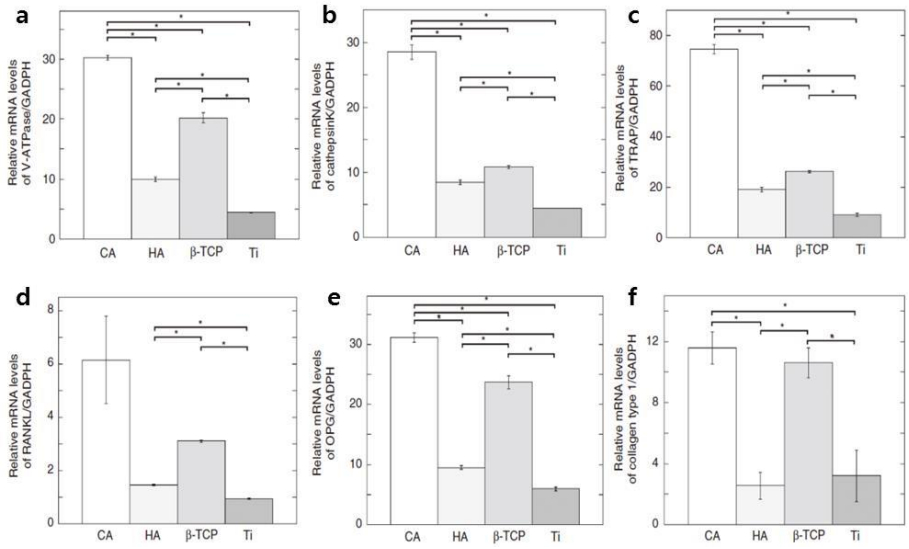

Figure 1.4 Activity of osteoclast and osteoblast on various bone implant substrate. **a-c,** Real-time PCR analysis of osteoclast markers. **a,** V-ATPase. **b,** Cathepsin K. **c,** TRAP. **d-e,** Real-time PCR analysis of osteoblast markers. **d,** RANKL. **e,** OPG. **f,** Collagen type 1 [36]

1.2.3 Synthesis methods of carbonate hydroxyapatite

Because of its great possibility for good bone graft material, there are many methods to synthesize carbonate hydroxyapatite. Carbonate hydroxyapatite can be synthesized through mechanochemical method, precipitation method, and sol-gel method[35-40]. In case of mechanochemical synthesis, calcium carbonate ($CaCO_3$), dicalcium phosphate dihydrate (DCPD), and urea aqueous solution were used as starting materials[38]. In the precipitation methods, general calcium reagent and phosphate reagents were used as the starting chemicals, but carbon containing chemical such as high concentration CO_2 gas[35], Na_2CO_3[36], NH_4HCO_3[39] was added during the synthesis procedure. In addition, ethanol (C_2H_5OH) was used as a carbon source of carbonate group in the sol-gel fabrication method[40]. All fabrication methods are similar to HAP synthesis methods, but the difference is using carbon containing reagent during the process.

1.3 Carbon capture and storage (CCS)

1.3.1 Atmospheric CO_2 concentration and current status

These days, atmospheric carbon dioxide (CO_2), well-known a greenhouse gas, is commonly considered main contributor to environmental problems such as climate change, current sea level rise, and melting glacier. As shown in Figure 1.5, the atmospheric CO_2 concentration was increased sharply in past 2 centuries. Before the industrial revolution, the concentration was maintained under the 280ppm, but it is almost 400ppm now[41, 42]. This huge increment of atmospheric CO_2 concentration after the industrial revolution has been caused by CO_2 emission from fossil fuel combustion. Today, about 80% of global energy use relies on fossil fuel based power generation[43]. As a result, contribution of using fossil fuel to increasing CO_2 amount in the air is more than 90% now. If we use fossil fuel continuously and continue the emitting CO_2 to the air in same rate, CO_2 concentration will be above 500 ppm by the end of this century[42]. Then, this will cause more serious environmental problems, and can threaten our lives. Therefore, many methods to reduce the CO_2 concentration have great interest to reduce the CO_2 concentration in the air.

There are various methods to reduce emitted CO_2 amount to the air. First, CO_2 emission can be reduced by energy conservation and efficiency improvements. This method looks like the lowest-cost and short-term method

until now. This can be carried by improving vehicle fuel efficiency and reducing building energy use. Another method is using alternative energy instead of fossil fuel. Many alternative energy sources have been reported such as solar, wind, biomass, and others. However, their efficiency is very low, and unit price for generating energy is expensive compared to fossil fuels[44]. In addition, those alternative energies are influenced by surrounding condition like weather and topography. Although we have many methods for using clean energy, many improvements are required. For example, the car using battery or hydrogen fuel for energy source were developed already, but it is hard to commercialize those cars because of low performance and safety issues. In addition, fuels made from biomass can be used to existing car, but the unit cost of production of those fuels is expensive[44]. The last method is carbon capture and storage method. By using this method, we can continue to use fossil fuel as energy source.

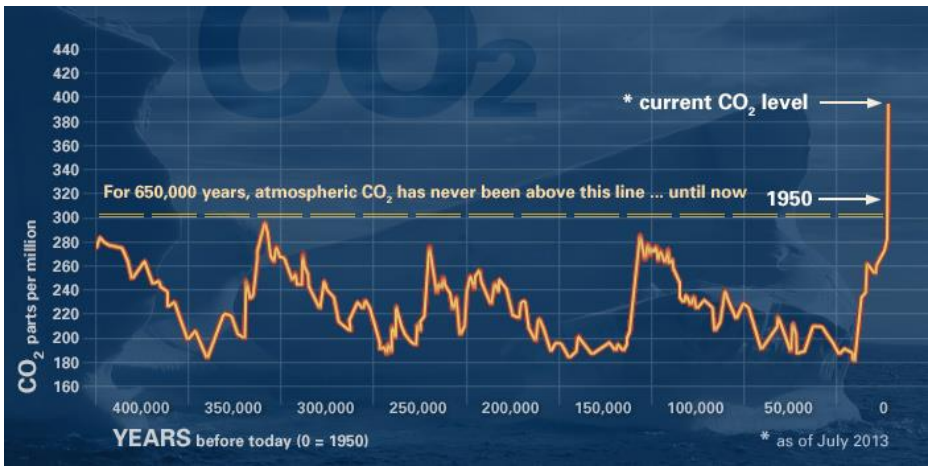

Figure 1.5 Atmospheric CO_2 concentration plot. This plots atmospheric CO_2 concentration synthesizing ice core proxy data 650,000 years in the past capped by modern direct measurements[45].

1.3.2 Carbon capture & storage methods

Carbon capture and storage (CCS) is one of reducing emitted CO_2 methods by capturing waste CO_2 generated form large CO_2 emission sources like fossil fuel power plants[46]. In this method, captured CO_2 is transported to storage site, and stored to prevent the release of large amount of CO_2 into atmosphere. Through this method, carbon migration from fossil fuel to air can be reduced, and finally, increment rate of CO_2 amount in the air can be slowed.

Generally this method is composed of three processes[47]. First step is capturing CO_2 from the source. As shown in Figure 1.6, there are several technologies to capture CO_2 from the large point sources[43]. In the "post-combustion capture", CO_2 is absorbed after the fuel combustion. Generally, the regenerable liquid solvent such as amine sorbent is used to capture CO_2 in flue gas. In contrast, CO_2 can be removed from the fuel before the combustion. This is called "pre-combustion capture". Using a water-gas reaction, the fuel was changed into mixture of hydrogen and CO_2. Then, CO_2 is collected after the hydrogen consumption after generating energy. The last CO_2 removing technology is called "oxyfuel". In this method, fuel is combusted in the oxygen environment, not in the ambient air condition. In this condition, almost of oxygen was converted to CO_2, therefore, CO_2 concentration in flue gas is very high. This flue gas can be compressed directly. Thus, additional procedure is not necessary to separate CO_2 from the flue gas.

After the capturing CO_2, the CO_2 containing liquid is transported to a

storage site. The transportation was carried out through the pipelines[48]. Therefore, constructions for transportation pipelines are required in carbon capture and storage method. After the transformation, CO_2 was deposed to the storage site. Storage site is the site has large storage capacity, generally underground or deep ocean[43]. However the most recommended sites are deep saline aquifers, which also have large estimated storage capacity[49].

This CCS method has great potential to CO_2 migration reduction. According to IPCC reports, This CCS method will be able to decrease CO_2 emissions by between 15 and 55% until 2100[43]. However, the CCS method only can slow the increment rate of atmospheric CO_2 amount. Because the CO_2 is stable and long-living gas in the atmosphere, decreasing CO_2 amount in the air would not be achieved through this technology[50]. If the CCS efficiency could be improved and absorbed 100% of emitted CO_2, restoring CO_2 concentration to pre-industrial concentration would take very long time.

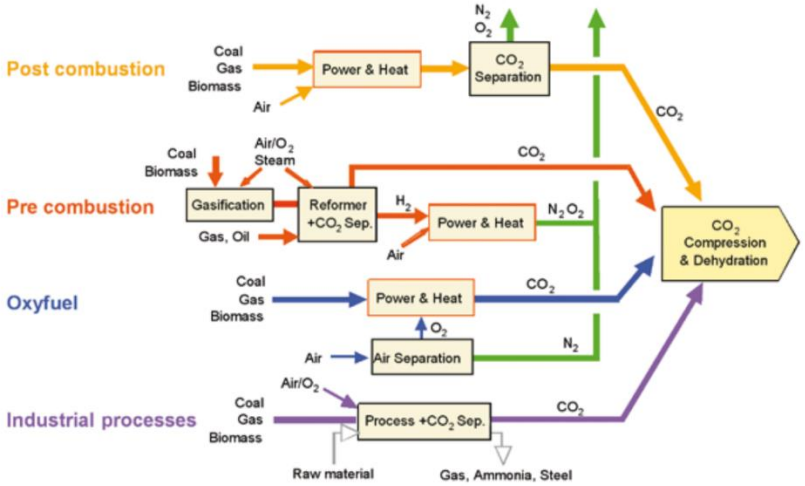

Figure 1.6 A schematic diagram of the main capture processes and systems[43].

1.3.3 Air capture

Currently, most studies related to CCS technology focused on capturing CO_2 in flue gas generated form fossil fuel combustion. However, there is "air capture" method capturing CO_2 directly from the atmosphere[51]. This method has several advantages compared to CCS method mentioned above[41]. Because CO_2 can be captured in everywhere, the capture system can be installed any place. Therefore, additional infrastructure such as pipe for transporting CO_2 liquid to storing site is not required in air capture method. In addition, already emitted CO_2 to the air can be absorbed through air capture method. It is very hard to apply CCS system to small CO_2 emission source such as transportation, small building, and home[52]. However, air capture can capture these kinds of CO_2. In summary, air capture has advantages in installation place, cost for constructing system, and CO_2 emission source scale compared to CCS method. Therefore, air capture is of great interest in CO_2 capturing research area.

Considering net CO_2 emission in each method, CCS release CO_2 as a result. CCS can reduce CO_2 emission, but not stop the emission. Even if all CO_2 can be captured through the CCS method, current large atmospheric CO_2 amount would maintain and will cause serious environmental problem for a long time. However, net CO_2 emission of air capture is negative. It can absorb CO_2 without generating the greenhouse gas. Therefore, atmospheric CO_2 level can be decreased if air capture is used. Without using air capture, it will take

centuries to restore atmospheric CO_2 level to pre-industrial level. However, there are few challenges in air capture method[53] The method should absorb CO_2 separately with desired amount of CO_2. In addition, cost of material used in air capture should not be expensive.

1.4 Carbonation of metal hydroxide sorbents

1.4.1 Alkali/Alkali earth metal hydroxide sorbents

It is known that metal hydroxide, especially alkaline hydroxide and alkali earth metal hydroxide, sorbents can capture CO_2 directly from the air in ambient condition[54-56]. In this method, atmospheric CO_2 is removed by carbonation reaction producing CO_3 ions in the solution. This reaction is easily observed through simple experiment by blowing CO_2 containing gas to calcium hydroxide ($Ca(OH)_2$) solution. The solution becomes cloudy because of generated $CaCO_3$ particles. Related to this experiment, a CO_2 capture system using $Ca(OH)_2$ solution is reported[57]. In this study, the pools of Ca(OH)2 saturated solution was prepared and wind blows across the surface. Then, solid $CaCO_3$ was formed and collected from the saturated solution. This result demonstrates that CO_2 can be efficiently captured in the ambient condition by using alkali earth metal hydroxide sorbent.

Generally, sodium hydroxide (NaOH) and calcium hydroxide ($Ca(OH)_2$) sorbent have been reported for atmospheric CO_2 capture[58, 59]. As shown in Figure 1.7a, both $Ca(OH)_2$ and NaOH capture CO_2 very well. However, NaOH solution has been more frequently reported than $Ca(OH)_2$. As shown in Figure 1.7b, the absorption rate is higher in case of NaOH solution. In addition, water loss is less in NaOH sorbent because of its lower vapor pressure[61], and it can be more efficient contacting system because of

higher concentrations of hydroxide[62]. NaOH also has some drawbacks. After the CO_2 absorption, NaOH changes to Na_2CO_3, which is soluble in the water[63]. Therefore, the status for the storage of this chemical would be liquid form which is not good for storage because of its large volume. The mineralized form Na_2CO_3 can be precipitated by drying water in the solvent. However, this process requires additional energy. In this respect, $Ca(OH)_2$ has advantage compared to NaOH.

To overcome drawbacks of each chemical, a new method was proposed[56]. Both NaOH and $Ca(OH)_2$ were used in this method. A scheme of this suggested capturing process is shown in Figure 1.8. First, NaOH was used as an alkaline liquid sorbent to remove atmospheric CO_2. Then, Na_2CO_3 solution is mixed with $Ca(OH)_2$ to produce NaOH and $CaCO_3$. In this process, the carbonate anion transferred from the sodium ion to the calcium cation. The efficiency of CO_3 ion transfer was about 94%. Therefore, this method keep absorption rate of NaOH, and atmospheric CO_2 mineralization ability of $Ca(OH)_2$. Another advantage of this capturing method is possibility of reusing NaOH. A drawback of this capturing process is this process is composed of 2 steps. This cumbersome method can be replaced by $Ca(OH)_2$ solution if CO_2 absorption rate of the solution is enhanced.

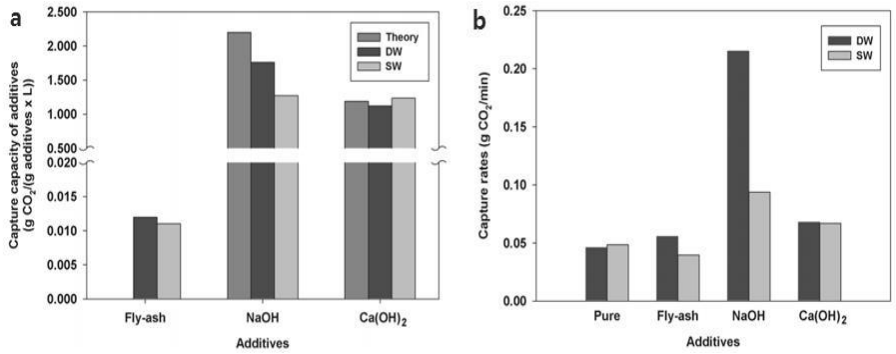

Figure 1.7 CO_2 capture capacity of each absorbent and capture rates of each absorbent. **a,** CO_2 capture capacity of each absorbent in distilled water and seawater. **b,** capture rates of each absorbent in distilled water and seawater. DW; distilled water, SW; seawater.[60]

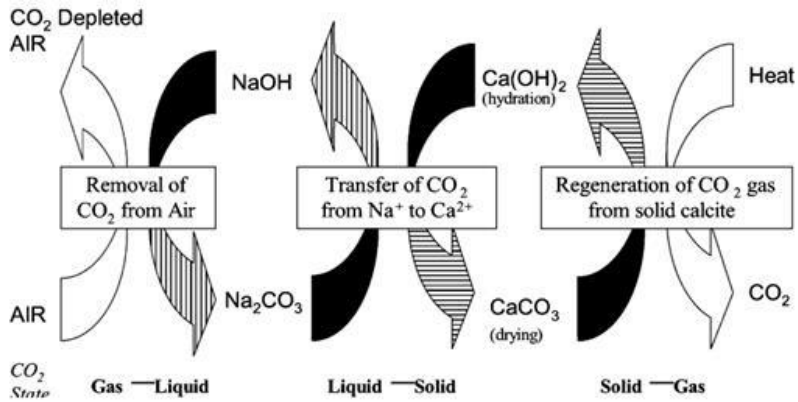

Figure 1.8 Overview of suggested efficient air extraction process. Capturing process and CO_3 ion transfer process was shown.[56]

1.4.2 Superoxide effect

It has been reported that superoxide radical enhanced CO_2 capture ability of alkali/alkali earth metal oxide[69]. As shown in Figure 1.9a, CO_2 absorption ability of NaOH was dramatically increased when H_2O_2 was added. To figure out how H2O2 can influence CO_2 absorption ability of NaOH solution, radical detection analysis was carried out. Then, it is confirmed that superoxide anion radical was generated after the H_2O_2 addition to the NaOH solution. To confirm the superoxide anion radical effect, superoxide dismutase (SOD) was used. Since SOD act as free radical scavenger, generated superoxide cannot influence to CO_2 absorption if SOD is exist[64]. In this experiment, the SOD added sample did not show difference from the NaOH solution itself, as shown in Figure 1.9b. This result demonstrated that superoxide enhanced CO_2 absorption ability of NaOH solution.

It is also reported that peroxide and superoxide is generated in $Ca(OH)_2$ solution after the H_2O_2 addition[65-67]. Based on these studies, H_2O_2 addition could enhance the CO_2 capturing ability of $Ca(OH)_2$ solution. Comparing reported value of CO_2 capturing ability of $Ca(OH)_2$, 1g of $Ca(OH)_2$ can absorb 0.03g of atmospheric CO_2 in the $Ca(OH)_2$ saturated solution, but it can capture 0.05g of CO_2 in H_2O_2 added solution[68,69]. Therefore, these results demonstrated that CO_2 absorption ability can be improved by generating superoxide radical in alkali/alkali earth metal hydroxide solution.

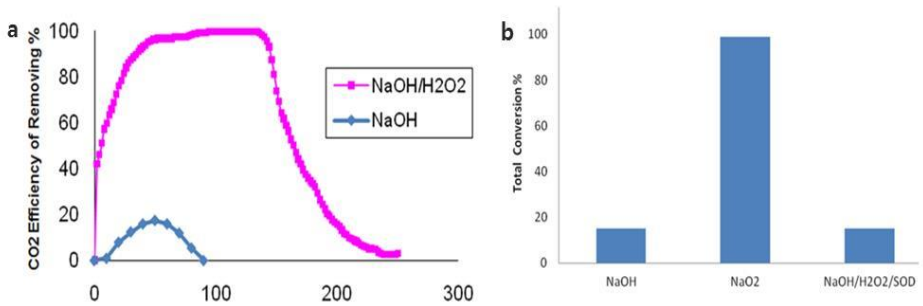

Figure 1.9 Superoxide anion radical effect on CO_2 absorption in the NaOH solution. SOD: superoxide dismutase. **a,** H2O2 effect on CO_2 absorption ability of NaOH solution. **b,** Superoxide anion effect confirmation.[69]

1.5 Research scope and design

In bone implant material research area, synthesizing biomaterial which is similar to natural bone is a big issue. The carbonate substituted hydroxyapatite (CHA) is of great interest because of its composition similarity with natural bone and potential to enhance bioactivity of bone grafts. In this regard, we introduced an innovative synthesis method for fabricating CHA which has similar chemical composition to natural bone.

In contrast with previously reported research, we used atmospheric CO_2 as a source of CO_3 ion in CHA. Most of previous research used carbon containing reagent for the CO_3 groups. However, atmosphere also has quite large amount of carbon. Because calcium hydroxide ($Ca(OH)_2$), generally used as starting material for hydroxyapatite (HAP) synthesis, can absorb atmospheric CO_2, $Ca(OH)_2$ was used as a starting material for our CHA synthesis.

Since the carbonation rate of $Ca(OH)_2$ is too slow to absorb enough CO_2 for CHA synthesis, hydrogen peroxide (H_2O_2) was added to the $Ca(OH)_2$ suspension for accelerating CO_2 absorption rate. After that, CHA particle synthesis was carried out. Because products of H_2O_2 decomposition are water and oxygen, adding H2O2 will not pollute the synthesized CHA nor generate impurity.

The synthesis was carried out in the aqueous solution via wet precipitation method. Advantages of wet precipitation method are regular

particle size of product and simplicity of the process. Therefore, precipitation method was selected for CHA formation. Washing procedure after the synthesis can be skipped by conducting precipitation in the water. Hence, water was used for the solvent of synthesis.

In summary, we tried to synthesize pure CHA having similar chemical composition to bone through atmospheric CO_2 absorption and wet precipitation method in this research.

Chapter 2. MATERIALS AND EXPERIMENTS

2.1 Sample preparation of carbonate hydroxyapatite

2.1.1 Materials

For the carbonate hydroxyapatite synthesis, calcium hydroxide ($Ca(OH)_2$, 99.0%) was purchased from KOJUNDO CHEMICAL LABORATORY company as a calcium reagent. In addition, hydrogen peroxide (H_2O_2, 30.0%) and phosphoric acid (H_3PO_4, 85.0%) were purchased from DAEJUNG chemicals as radical generating reagent and phosphate reagent, respectively.

2.1.2 Synthesis of carbonate hydroxyapatite

Carbonate hydroxyapatite (CHA) was synthesized using wet precipitation method. First, 100ml of 1M $Ca(OH)_2$ aqueous solution was prepared, and the suspension was vigorously stirred and sonicated for 20 minutes to make the suspension uniform. Then, 100ml of H_2O_2 solution was added. Again, sonication and stirring was applied for 10 minutes. After that,

100ml of 0.6M H_3PO_4 aqueous solution was added while vigorously stirring. The precipitates were aged for 4 hours and then collected using filter-press method. The precipitants were oven-dried at 60℃ overnight. The scheme of this precipitation process was shown in Figure 2.1. All procedures were carried out in ambient condition.

For the comparison between synthesized CHA and hydroxyapatite (HAP), HAP was also synthesized using wet precipitation. 500ml of 1M $Ca(OH)_2$ aqueous solution and 500 ml of 0.6M H_3PO_4 aqueous solution were prepared. The $Ca(OH)_2$ solution was sonicated and stirred for 30 minutes. Then, H_3PO_4 solution was added to the $Ca(OH)_2$ solution with a constant rate, 12.5ml/min, using digital burette. After the 24 hour-aging time, the precipitates were collected and dried in same way as mentioned above.

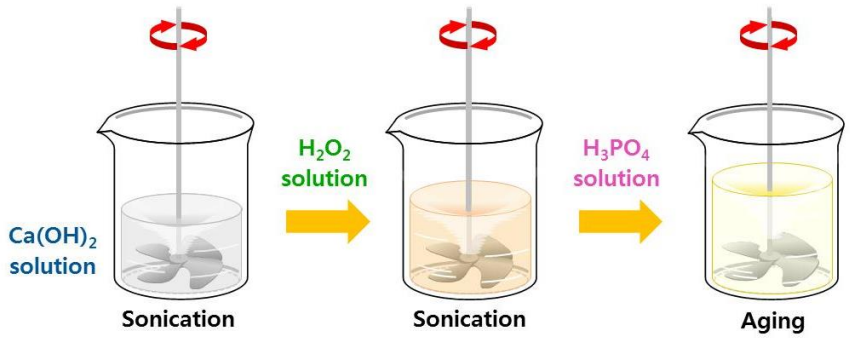

Figure 2.1 Experimental set-up for synthesizing carbonate hydroxyapatite (CHA). Hydrogen peroxide (H_2O_2, 30%, 100ml) was added into 100 mL of calcium hydroxide solution ($Ca(OH)_2$, 1M). Then, phosphoric acid solution (H_3PO_4, 0.6M, 100ml) was added to the suspension. The solution was vigorously stirred for 4 hours.

2.1.3 Amount modification of substituted carbonate in carbonate hydroxyapatite

To determine the effect of H_2O_2, the radical generating reagent, on the carbonate (CO_3) substituted amount, three samples were prepared. Same amount and concentration of $Ca(OH)_2$ solution and H_3PO_4 solution were used in the each sample preparation, but added amount of H_2O_2 solution was changed.

To make all the synthesis systems have equal final volume, added H_2O_2 solution were made by mixing distilled water and 30% H_2O_2 solution with different ratios. The mixing ratios of distilled water and H_2O_2 solution were shown in Table 2.1. This 100ml of appropriate concentration of H_2O_2 solution was added to the vigorous stirred and sonicated $Ca(OH)_2$ solution, then H_3PO_4 solution added. The synthesis process was conducted in the same way as explained before.

Table 2.1 Mixing amount of distilled water and H_2O_2 solution for different sample preparation

Sample	Mixing amount	
	Distilled water	H_2O_2 solution
3% H_2O_2	80ml	20ml
7.5% H_2O_2	50 ml	50 ml
15% H_2O_2	0 ml	100 ml

2.2 Characterization

2.2.1 Powder X-ray diffraction (XRD)

To analyze the crystal structure and phase, powder X-ray diffraction (XRD) was carried out on a D-8 advance X-ray diffractometer with Cu Kα radiation (λ=1.54056Å). The sample was prepared through following steps. Precipitated powder was oven-dried and ground well using alumina mortar. The well-ground powder was carefully loaded on silicon holder, and the measurement was conducted. XRD patterns were recorded in a range of 5~60° with scan rate 1°/min. Obtained XRD patterns were compared with previously reported JCPDS cards.

2.2.2 Field emission scanning electron microscopy (FESEM)

The morphology and size of CHA particles was characterized with field emission scanning electron microscopy (FESEM, Supra 55VP & Sigma, Carl Zeiss). Before observation, all samples were fixed on the stubs by carbon tape. Then platinum coating was carried out using Pt sputter for optimal electron conductivity to prevent charge-up phenomena. Images were taken with an acceleration voltage of 2.00kV.

2.2.3 Fourier transform infrared spectroscopy (FT-IR)

Fourier transform infrared spectroscopy (FT-IR) spectra were obtained using a FT-IR spectrometer (Nicolet iS10, Thermo scientific). FT-IR analysis was conducted to confirm the CHA fabrication. As-synthesized particles were sampled as KBr pellet for measurement. 0.02g of powder was ground with 1.98g of KBr, and 0.1g of sample was pressed to make the powder sample in a pellet form. The samples are scanned under the ambient condition with scan range from 400cm^{-1} to 4000cm^{-1}. Total 32 cycles of scans were carried out for each sample.

2.2.4 Element analyzer

Element analyzer (Flash 2000, Thermo scientific) was used for calculating the amount of substituted carbonate groups in CHA lattice. The precipitated CHA were well ground using alumina mortar. Samples were introduced directly into the tin container of element analyzer using spatula. Then, amount of carbon atom in the sample was measured.

2.3 Carbonation confirmation

2.3.1 Electron paramagnetic resonance (EPR)

Electron paramagnetic resonance (EPR) measurements were carried out at KBSI, Seoul, Korea. EPR was performed using a Bruker EMX/Plus spectrometer. EPR spectra of the spin adducts were conducted on a Bruker EMX spectrometer operating at room temperature, a microwave frequency 9.64GHz, and a 100-kHz field modulation. EPR measurement was carried out for radical detection. To confirm the radical involvement for the CO_2 absorption, 5,5-Dimethyl-1-pyrroline-N-oxide (DMPO, Aldrich, USA) was used as the spin trapping reagent. DMPO can trap superoxide radical ($O_2^{\bullet-}$) and hydroxyl radical (•OH), and DMPO/•OOH and DMPO/•OH adducts is formed, respectively[70]. Chemical structure of these DMPO adducts were shown in Figure 2.2. Since each DMPO adducts has specific spectra, radical existence and species can be analyzed through the EPR measurement. For the measurement, 4μl of sample was added to 36μl of distilled water, then, 2μl of DMPO was added before the measurement. The small amount of this solution was transferred to a glass tube, and the EPR measurement was conducted.

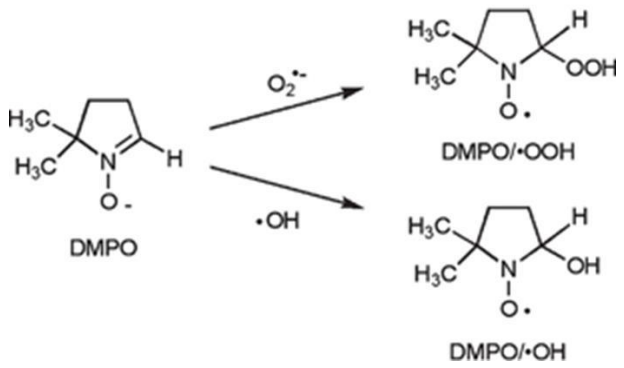

Figure 2.2 Chemical structure of 5,5-Dimethyl-1-pyrroline-N-oxide (DMPO) and DMPO adducts. When DMPO trapped superoxide radical ($O_2^{\bullet-}$), DMPO/•OOH is formed, and DMPO/•OH adducts is formed when DMPO trapped hydroxyl radical (•OH)[70].

2.3.2 Gas chromatography

To confirm the carbonate in synthesized CHA came from the atmospheric CO_2, gas chromatography (GC) was carried out to detect CO_2 absorption during the synthesis. 2mg of $Ca(OH)_2$ was put into the 250ml round bottom flask, and the flask was sealed with septum. Then, 5ml of distilled water and 5ml of H_2O_2 solution was added. 1ml of air in the flask was extracted using GC syringe, and CO_2 amount in the gas was analyzed. To measure the CO_2 amount change in the flask, sampling was carried out with different reaction time.

2.4 Stability of synthesized carbonate hydroxyapatite

2.4.1Solubility test

To examine the stability of synthesized CHA in various pH conditions, solubility test was conducted. 0.5g of CHA powder was dispersed in 50ml of pH 12 sodium hydrogen phosphate/sodium hydroxide buffer at room temperature. To observe the stability of the powder, the experiment was carried out for different aging time. In addition, 0.5g of CHA powder was dispersed in 50 ml of H_3PO_4 solution, which were titrated at pH 4 to figure out stability of CHA in acidic environment. The experiment was also carried out

for different aging time like the stability test using basic solution (pH 12). Then, the remaining amount of the powder from each pH condition was measured accurately by weight to compare its solubility in acidic/basic environment. Each sample was analyzed in fourfold (n=4).

Chapter 3. RESULT AND DISCUSSION

3.1 Material characterization

3.1.1 Characterization of carbonate hydroxyapatite

3.1.1.1 XRD and SEM studies

The XRD pattern of our synthesized CHA is shown in Figure 3.1. It is possible to verify the spectrogram aspect of synthesized CHA by using International Center for Diffraction Data (ICDD). Our CHA was slightly amorphous and showed characteristic peaks of carbonate hydroxyapatite according to the ICDD PDF number 00-019-0272. There is no other phase was appeared except carbonate hydroxyapatite. Therefore, we confirmed that carbonate hydroxyapatite was successfully synthesized via our wet precipitation method.

To distinguish our synthesized CHA from the HAP, we provided evidence of the existence of CO_3 in the CHA structure. To compare CHA and HAP, HAP sample was also prepared. We synthesized HAP using precipitation method, and XRD analysis was conducted. As shown in Figure 3.2a, peaks of synthesized HAP were well matched to peaks of hydroxyapatite,

according to the ICDD PDF number 01-073-0293. It has more crystalline compared to our CHA. Because no other phase was exist, the XRD analysis of our synthesized HAP demonstrated that pure HAP was formed.

Next, the XRD peak positions of CHA and HAP samples were carefully compared. In Figure 3.2b, the XRD peaks shifted toward higher angular positions as the CO_3 substituted into the HAP structure. It is known that the *a* lattice parameter decreases with increasing amount of substituted carbonate for B-type carbonated apatites, while the *c* lattice parameter increase[1]. This trend was also observed in the comparison of HAP and CHA ICDD PDF file. The *a* lattice parameter decreased from 9.432 Å to 9.309 Å, and the *c* lattice parameter increased from 6.881 Å to 6.927 Å. As d-spacing value is calculated according to the following equation, different lattice parameter values cause the different d-spacing value if the (h k l) value is same.

$$\frac{1}{d^2} = \frac{4}{3}\left(\frac{h^2 + hk + k^2}{a^2}\right) + \frac{l^2}{c^2}$$

Because the compared (h k l) values of the peaks in Figure 3.2b are (2 0 0) and (2 1 1) respectively, *a* parameter contributes more to *d* value change than *c* parameter. Therefore, *d* value became smaller as more CO_3 is substituted into the CHA lattice. Because θ is decided by Bragg's law, $n\lambda = 2d\sin\theta$, θ value increase as d value decrease. For such a reason, XRD

peaks of CHA shifted toward higher angular position. This analysis results clearly demonstrate that our synthesized CHA has CO_3 groups in its structure. Therefore, it could be distinguished from HAP.

In Figure 3.3, the morphologies of the synthesized HAP and CHA are illustrated. The synthesized HAP particles were homogeneous, with rice shapes and size of approximately 80nm, as shown in 3.3a. However, the morphology of our synthesized CHA is totally distinct from that of HAP. In Figure 3.3b, our CHA has a flower-like morphology with the size of 100nm, having narrow particle size distribution. Comparison of the product morphologies in Figure 3.3 implied that the H_2O_2 affects the morphology of particles during the particle formation.

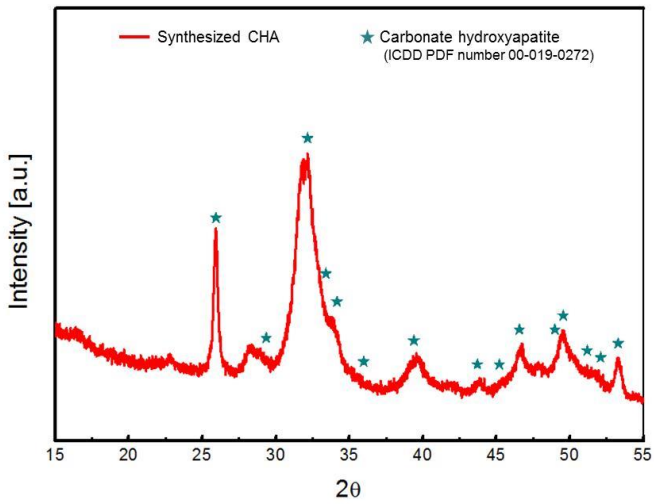

Figure 3.1 XRD pattern of synthesized carbonate hydroxyapatite (CHA). CHA was synthesized well and it is slightly amorphous.

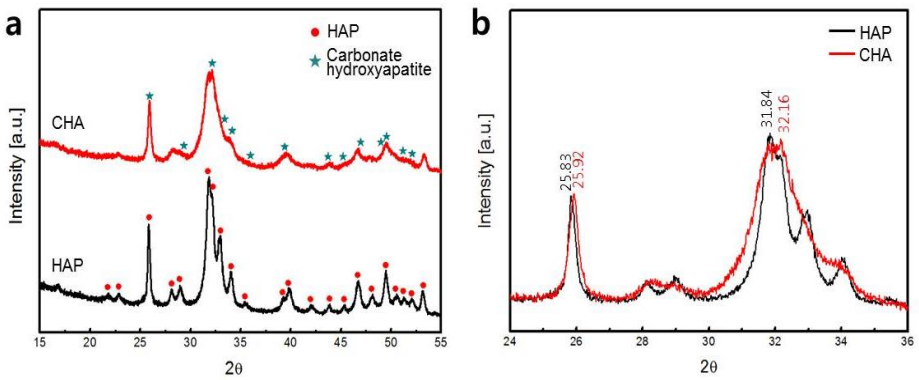

Figure 3.2 Distinction between carbonate hydroxyapatite (CHA) and hydroxyapatite (HAP) **a,** HAP was synthesized in pure form, and this pure HAP was used for the comparison with CHA. **b,** XRD peaks of CHA is located at higher angular position, and this indicates that carbonate groups are in its chemical structure.

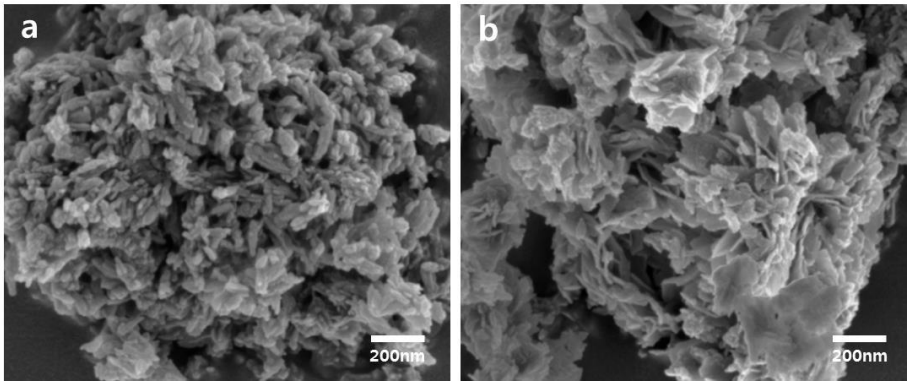

Figure 3.3 Field emission scanning electron microscopy (FESEM) image of synthesized hydroxyapatite (HAP) and carbonate hydroxyapatite (CHA). **a,** The HAP particle has rice shape with size of approximately 80nm. **b,** The CHA particle exhibits the flower-like morphology with the size of 100nm The FESEM image shows that both materials have narrow particle size distribution.

3.1.1.2 FT-IR studies

Figure 3.4 shows FT-IR spectrum of synthesized CHA through wet precipitation method. The all infrared band positions and their assignments are shown in Table 3.1. The spectrum indicated that our CHA has CO_3 substitution. The peaks appearing at wave number values of 873, 1420, and 1482 cm^{-1} demonstrated that the carbonate ion substitution in CHA lattice. The broad band appeared at 1638 and 3440 cm^{-1} indicate adsorbed H_2O in the materials. The band of structural OH which appears at around 3565 cm^{-1} is scarcely visible because the band at 3440 cm^{-1} which is due to adsorbed water overlaps the weak band of structural OH. In addition, we further analyze our FT-IR spectrum to check whether our CHA is A-type carbonate hydroxyapatite, OH ion site is substituted by CO_3 ion, or B-type hydroxyapatite, PO_4 ion site is substituted by CO_3 ion. According to reported sesult[71], our CHA can be considered as B-type. However, it cannot entirely exclude the possibility of A-type carbonate apatite fractions. The fraction of A-type and B-type could be calculated through the peak area comparison[72]. Because the typical peak of A-type CHA is 880 cm^{-1} and that of B-type is 872 cm^{-1}, the presence of CO_3 substituting in the OH site or PO_4 can be evaluated by the peak area ratio[1]. The calculated A/B ratio of our CHA is about 0.4. Therefore, our CHA can be regarded AB-type carbonate hydroxyapatite like natural bone.

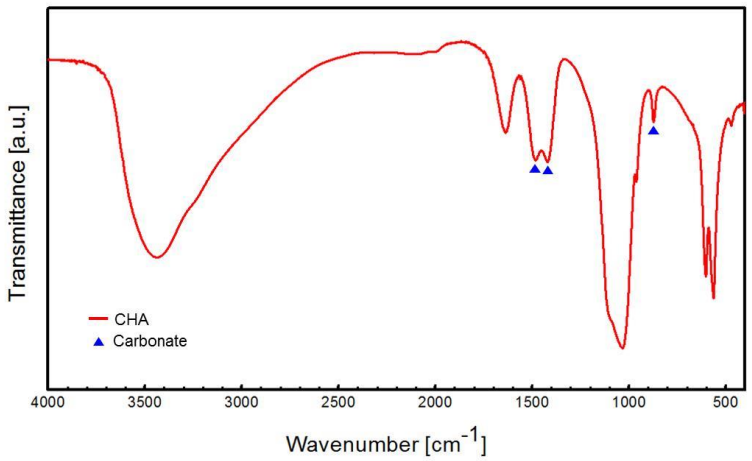

Figure 3.4 Fourier transform infrared (FT-IR) spectrum of synthesized carbonate hydroxyapatite (CHA). Peaks of carbonate appeared in the CHA spectrum, indicating carbonate substitution occurred.

Table 3.1 Assignments of the observed vibrational of synthesized carbonate hydroxyapatite (CHA)

Assignments	Observed vibrational frequencies (cm^{-1})
PO_4 bend v_2	471
PO_4 bend v_4	563
PO_4 bend v_4	603
CO_3 group v_2	873
PO_4 bend v_1	961
PO_4 bend v_3	1031
PO_4 bend v_3	1096
CO_3 group v_3	1420
CO_3 group v_3	1482
H_2O adsorbed v_2	1638
H_2O adsorbed	3440
OH stretch	3744

3.1.2 Solubility of carbonate hydroxyapatite

We also observed stability of our CHA in acidic and basic environments. First, we measured the pH of our CHA in distilled water because it is known that the pH affect bone regeneration ability[73]. It was reported that the osteoblast viability was significantly enhanced in the slightly basic environment, range from pH 8.0 to 8.5[73]. The measured pH value of precipitated CHA was about 8.6, and this value is very close to the optimum pH level. Next, we compared the remaining amounts of CHA in the acidic aqueous solution (pH 4.0) and basic aqueous solutions (pH 12.0) at room temperature with different aging time. Our CHA maintained its phase even after 1 week aging time in the pH 4.0 and pH 12.0 as shown in Figure 3.5. The Figure 3.6 demonstrated that our CHA is quite stable in acidic environment and basic environment, but slightly soluble in both condition. After 1 week aging in those solutions, the remaining amounts of CHA decreased from 0.5000 g to 0.4545g and 0.4585g in acidic and basic environment respectively. This demonstrated that our CHA is more stable in basic environment.

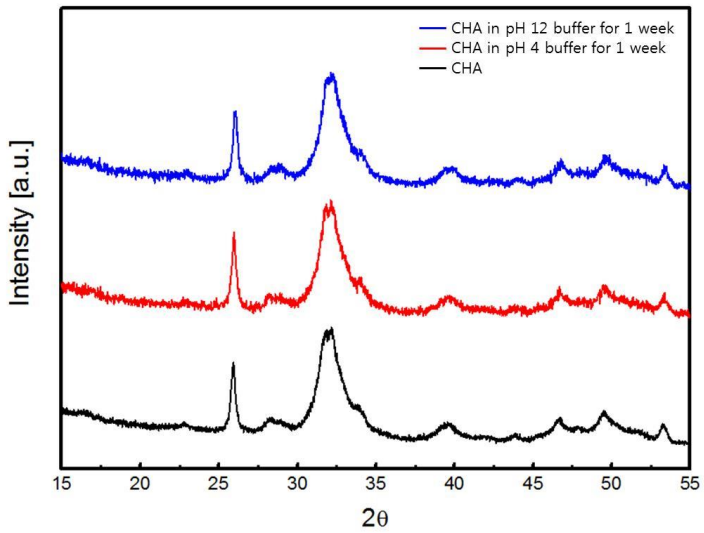

Figure 3.5 Stability test of carbonate hydroxyapatite (CHA) in acidic/basic solution for a week. CHA maintained its phase after aging in pH 4 and pH 12 solution at room temperature for a week.

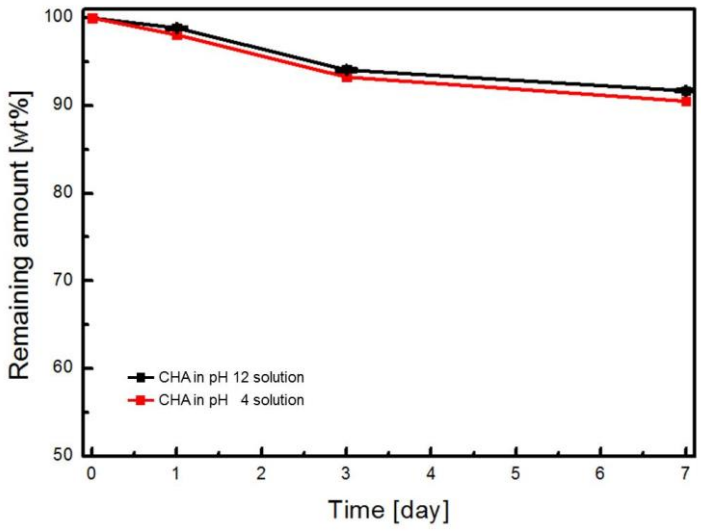

Figure 3.6 Solubility test of carbonate hydroxyapatite (CHA) in the acidic pH and basic pH condition. The remaining amounts of CHA after various aging time were compared.

3.2 CO_2 absorption during the process

3.2.1 CO_2 absorption from the air

Although we did not add any carbon containing reagent during the synthesis, CHA was successfully synthesized through our synthesis method. Therefore, we supposed that carbon in substituted CO_3 group of CHA might come from atmospheric CO_2. To prove our claim, we conducted gas chromatography experiment and analyzed CO_2 amount change during the reaction. To calculate exact absorbed amount of CO_2, the experiment was carried out in the closed system using a sealed round flask. Figure 3.7 demonstrated that our system really absorbed CO_2 from the air. CO_2 in the ambient air started to be absorbed into the solution immediately after the H_2O_2 solution was added to $Ca(OH)_2$. The amount of CO_2 continuously decreased as the reaction progressed. The absorption rate decreased over the reaction time. This is supposed because of decreased ion in the solution which can react with atmospheric CO_2. When we conducted the experiment using 25 μmol of $Ca(OH)_2$ and H_2O_2, the CO_2 amount changed from 9 μmol to 3 μmol in 10 minutes. This CO_2 capturing efficiency is much higher than reported previously. It was reported that 1 liter of saturated $Ca(OH)_2$ solution can capture 2.25g of CO_2 in 30% CO_2 environmant[68]. Changing to same unit, 1 liter of our $Ca(OH)_2$ solution with H_2O_2 can absorb 0.0132g of CO_2 in ambient condition. Since ambient air has 0.04% CO_2, the absorbed CO_2 amount was

very large. This high CO_2 absorption ability in our system is assumed because of added H_2O_2. It is known that CO_2 can be swiftly attacked by nucleophiles[69]. Generally, H_2O_2 generates reactive oxygen species, the strong nucleophiles, when it decomposed. Therefore, it seems like that CO_2 is absorbed to the suspension efficiently because of generated reactive oxygen species. The GC result showed that atmospheric CO_2 was absorbed during the synthesis efficiently in the ambient condition. In addition, the result indicated that CO_2 is the source of carbonate group in CHA.

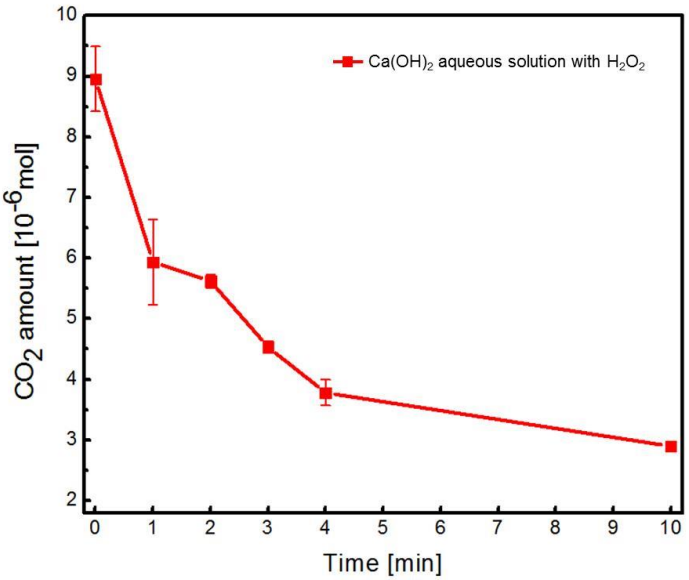

Figure 3.7 Change of the carbon dioxide (CO_2) amount in the closed flask. The amount of CO_2 decreased as the reaction progress.

3.2.2 Confirmation of radical formation

To confirm the involvement of reactive oxygen species during CO_2 capture process, we carried out electron paramagnetic resonance (EPR) experiment. As shown in Figure 3.8, reactive oxygen species were generated when H_2O_2 solution was added to the $Ca(OH)_2$. The generated reactive oxygen species were hydroxyl radical and superoxide anion radical. Compared to the control, much larger amount of hydroxyl radical was generated in the $Ca(OH)_2$ and H_2O_2 blending suspension. Interestingly, superoxide radical was generated only in the $Ca(OH)_2$ and H_2O_2 mixing solution.

Generally, aqueous superoxide is not considered appropriate agent for CO_2 capture because of its rapid hydrolysis and disproportionation in water. However, superoxide anion can be formed spontaneously by blending $Ca(OH)_2$ with H_2O_2. The formation of superoxide is carried on in two steps. First, calcium peroxide (CaO_2) was formed, and then superoxide was generated via interaction between peroxide and H_2O_2[74].

$$Ca(OH)_2 + H_2O_2 \rightarrow CaO_2 + 2H_2O$$

$$CaO_2 + 2H_2O_2 \rightarrow Ca(O_2)_2 + 2H_2O$$

Through these reactions, the anion-radical is stabilized and can act as an effective nucleophile for CO_2 capture in the aqueous solution[69]. As a result,

this superoxide radical in the solution can attack and mineralize the atmospheric CO_2 through the following equation.

$$Ca(O_2)_2 + CO_2 \rightarrow CaCO_3 + 1.5O_2$$

This EPR result proved that superoxide anion was formed in the synthesis system, and the anion radical participated in the CO_2 capturing process. In conclusion, large amount of CO_2 was absorbed to our CHA synthesis system by adding H_2O_2, and generated superoxide anion radical contributed to CO_2 absorption for the source of substituted CO_3 in our CHA.

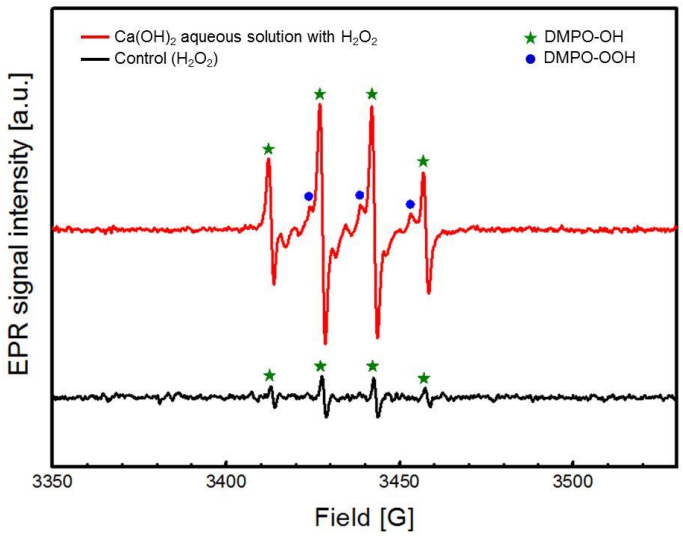

Figure 3.8 Electron paramagnetic resonance (EPR) analysis of control and $Ca(OH)_2$ blend solution. The result showed that superoxide radical was only generated in our system, and large amount of hydroxyl radical was generated when $Ca(OH)_2$ react with H_2O_2.

3.3 Phase transformation during carbonate hydroxyapatite formation

3.3.1 Phase transformation during the synthesis

We investigated kinetic mechanism how the CHA synthesized in our system. First, we tried to verify the CO_2 mineralization as mentioned above. Since we insisted that CO_2 mineralization was occurred after adding H_2O_2 into the $Ca(OH)_2$ solution, we checked the mineral phases of initial material ,$Ca(OH)_2$, and 10 minutes aging sample after adding H_2O_2. As shown in Figure 3.9, the characteristic peaks of $CaCO_3$ and CaO_2 were detected in the aged sample with adding H_2O_2. The result showed that all $Ca(OH)_2$ was transformed to $CaCO_3$ and CaO_2. To figure out how much amount of CO_2 was absorbed to the suspension, we measure the mass difference between used $Ca(OH)_2$ and CaO_2+$CaCO_3$ product. The increase mass was about 1g, and the calculated absorbed amount of CO_2 was 0.011 mol. This result corresponded to the CO_2 mineralization mechanism through the peroxide formation and superoxide formation. The result showed that fairly large amount of CO_2 was absorbed in the $Ca(OH)_2$ and H_2O_2 blending aqueous solution.

In Figure 3.10, XRD patterns of the intermediate phases after addition of H_3PO_4 to the $Ca(OH)_2$ and H_2O_2 mixed solution (CaO_2 and $CaCO_3$) were shown according to different aging time. In the initial stage with aging time 1 minute, the major phases were found to be dicalcium phosphate dehydrate

(DCPD), apatic structured phase, and CaO_2. As the aging time getting longer, peak of DCPD was disappeared in early stage. However, peak of CaO_2 appeared even in the 2 hours aging time. The characteristic peak of CaO_2 was disappeared after the 4 hours aging time. At the sample with 4 hour aging time, only the CHA phase was observed.

The powders were collected from the different aging time, and their morphologies are observed through the FESEM. The morphologies of the precipitants reflected the phase transformation process toward CHA. As shown in Figure 3.11 a and b, the large plate shape DCPD was observed. In addition, small amount of CHA particles were detected which was attached on the DCPD plate. After the 4 hours aging time, the plate shape DCPD was disappeared and only flower shape CHA was observed. Moreover, the crystallinity was slightly increased compared to the 2 hours aging time. This XRD result demonstrates that DCPD, which contains Ca and P in the ratio 1:1, in the intermediate phase during CHA synthesis. During aging time, DCPD gradually dissolved and act as the source of Ca ion and P ion for the CHA formation.

To comprehend phase transformation mechanism and H_2O_2 effect during the CHA synthesis, we conducted another experiment for CHA synthesis using $CaCO_3$ as the starting material. Since $CaCO_3$ was formed after the addition of H_2O_2 in to the $Ca(OH)_2$ solution, $CaCO_3$ based experiment could help to understand the H_2O_2 effect on the CHA synthesis. First, we added H_3PO_4 solution to $CaCO_3$ suspension without using H_2O_2. Other

procedures were progressed in the same way. As shown in Figure 3.12 a, only a small amount of apatic structured phase was synthesized, and $CaCO_3$ was not disappeared after 30 minutes aging time. The characteristic peaks of $CaCO_3$ were even appeared after 72 hours aging time. This result is very distinct from $Ca(OH)_2$ based CHA synthesis. While pure CHA was synthesized with 4 hours aging time in our $Ca(OH)_2$-H_2O_2 based CHA synthesis method, the CHA synthesis reaction was not completed in the $CaCO_3$ based synthesis without using H_2O_2. This indicated that there is H_2O_2 effect during the CHA synthesis. To figure out precisely, we conducted few more experiments. First, we used $CaCO_3$ and H_2O_2 blending suspension as starting material for the particle synthesis. In this experiment, all $CaCO_3$ peak was disappeared and HAP and CHA were synthesized within 30 minutes after the addition of H_3PO_4. We also carried out the experiment using washed $CaCO_3$ as the starting material. We prepared washed $CaCO_3$ particles via washing particles in the $CaCO_3$ and H_2O_2 blending suspension using distilled water. Interestingly, the result of this experiment was same as the result of using $CaCO_3$ based synthesis without H_2O_2. These results demonstrated that H_2O_2 contribute to phase transformation for CHA formation during the synthesis.

Based on XRD results and analysis, a scheme of carbonate hydroxyapatite synthesis mechanism was shown in in Figure 3.13. This figure also shows CO_2 absorption process. As shown in 3.13, added H_2O_2 influenced many steps. First, H_2O_2 participated in superoxide radical generation, and

involved to CO_2 absorption procedure. Next, H_2O_2 also participated in CHA particle precipitation. It made CHA formation possible by helping reaction between $CaCO_3$ and DCPD.

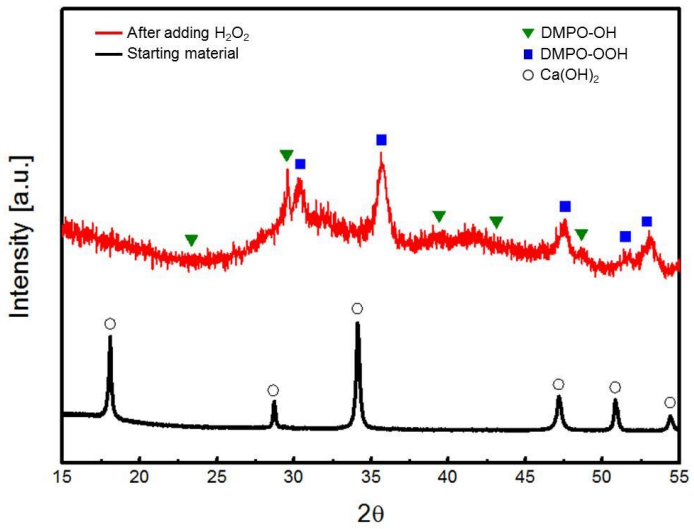

Figure 3.9 XRD analysis of the mineral phases before and after adding H_2O_2 solution to $Ca(OH)_2$ aqueous solution. H_2O_2 added sample was aged for 10 minutes after adding H_2O_2.

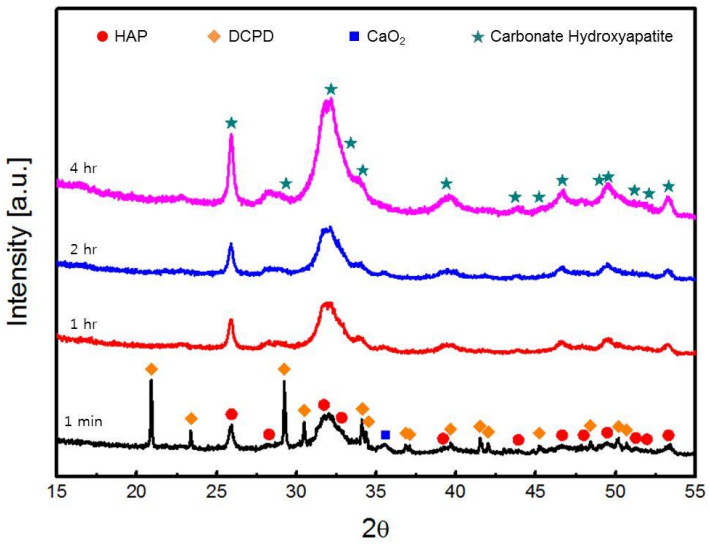

Figure 3.10 XRD patterns of intermediate phases during aging process for carbonate hydroxyapatite (CHA) synthesis. The aging time was measured from the complete addition of H_3PO_4 in the $Ca(OH)_2$ and H_2O_2 mixed solution.

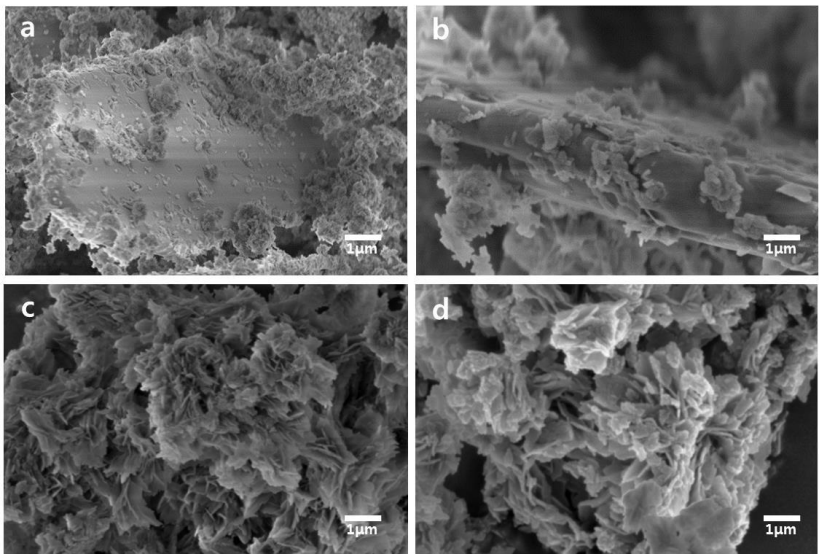

Figure 3.11 Morphologies of the intermediate phase of carbonate hydroxyapatite (CHA) during the synthesis. **a-b,** During initial stage, large platelet shape of dicalcium phosphate dihydrate (DCPD) was observed, and CHA particles are attached on the DCPD plate. **c-d,** after the 4 hour aging time, platelet shape of DCPD was gone, and only the flower-shaped CHA particles were left.

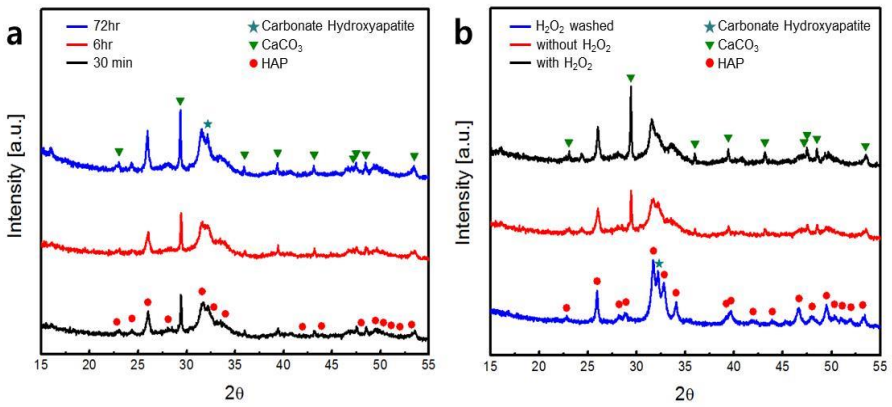

Figure 3.12 Confirmation of H_2O_2 effect through the comparison of intermediate phase in the $CaCO_3$ based synthesis system with and without H_2O_2. **a,** XRD patterns of the intermediate phases after addition of H_3PO_4 in the $CaCO_3$ without H_2O_2 with different aging time. Carbonate hydroxyapatite was not synthesized even after the 72 hours aging time when H_2O_2 was not added. **b,** XRD patterns of 30 minutes aging time samples with or without H_2O_2. The $CaCO_3$ peaks were disappeared only in the H_2O_2 added sample.

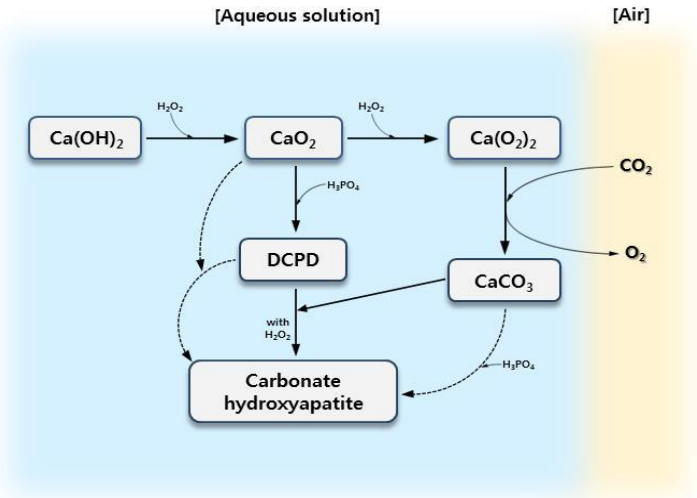

Figure 3.13 A scheme for carbonate hydroxyapatite (CHA) synthesis mechanism.

3.4 CO_3 substituted amount control

3.4.1 H_2O_2 amount effect

We verified that there was H_2O_2 effect on CO_2 capture. Therefore, we tried to figure out how the added H_2O_2 amount affect CO_3 substitution into the CHA lattice. Different amount of H_2O_2 was added to same amount of $Ca(OH)_2$ solution and other procedure were conducted in same way. Figure 3.13 showed that spectra of CHA which were synthesized with different H_2O_2 concentration. The signature peaks of CO_3 at 873, 1420, and 1482 cm^{-1} were labeled in the figure. The transmittance of those peaks diminished gradually with increasing added amount of H_2O_2. This qualitative increased amount of substituted CO_3 according to the higher concentration of H_2O_2 implied that we can control the substituted CO_3 amount by controlling used H_2O_2 amount.

To compare the substituted amount of CO_3 in synthesized CHA more precisely, we carried out quantitative analysis using element analyzer. The accurate amount of substituted CO_3 was shown in Table 3.2. Since the element analyzer can analyze carbon amount in weight %, substituted CO_3 amount was calculated based on measured carbon amount. The result of element analyzer showed the same tendency to the FT-IR result. Interestingly, only the samples which were synthesized with H_2O_2 have the values in the range of CO_3 wt % in natural bone, 2.3 to 8 wt%[4]. This result indicated that we can control the substituted CO_3 amount in the natural CO_3 substitution

Table 3.2 Carbon amount and calculated CO_3 amount in hydroxyapatite (HAP) and each carbonate hydroxyapatite (CHA) sample

Sample	C amount	CO_3 amount
0% H_2O_2 (HAP)	0.4394 wt%	1.5683 wt%
3% H_2O_2	0.5968 wt%	2.9818 wt%
7.5% H_2O_2	0.7561 wt%	3.7778 wt%
15% H_2O_2	0.7685 wt%	3.8396 wt%

range by controlling the blended H_2O_2 amount. Moreover, the synthesized CHA has similar chemical composition to natural bone.

The element analyzer result showed that 3.8396 % of total mass of CHA synthesized with 15% H_2O_2 concentration is CO_3 group. Since the mass of CHA, the final product, was 10.9g, the mass of CO_3 in CHA is 418.4mg. Based on this value, we can calculate how much amount of CO_2 was absorbed, and absorbed CO_2 mass was 306.8mg. It is known that the CO_2 concentration in air now is about 400ppm[75]. Transferring this CO_2 concentration to unit in mg/L, 0.8mg of CO_2 exists in a liter of atmosphere. This demonstrated that that our 0.3 liter of CHA synthesis system can absorb CO_2 in more than 380 liters of air.

In the FESEM analysis to compare the particle morphologies of HAP

and CHA particles, the shapes of those particles were very distinct from each other. To examine the H_2O_2 effect on particle morphology, we observed particles synthesized with different concentration of H_2O_2 using FESEM. In Figure 3.14, the morphologies of particles were shown. As the more H_2O_2 was added, more flower-shape particle was observed. In 3% H_2O_2 sample, rice shape particles and flower shape particles were mixed. However, less rice shape particles observed and most of particles had flower shape in 7% H_2O_2 sample. And finally, the rice shape particles disappeared and only flower shape particles were detected in 15% H_2O_2 sample. This demonstrated that added H_2O_2 also have influence on the particle shape.

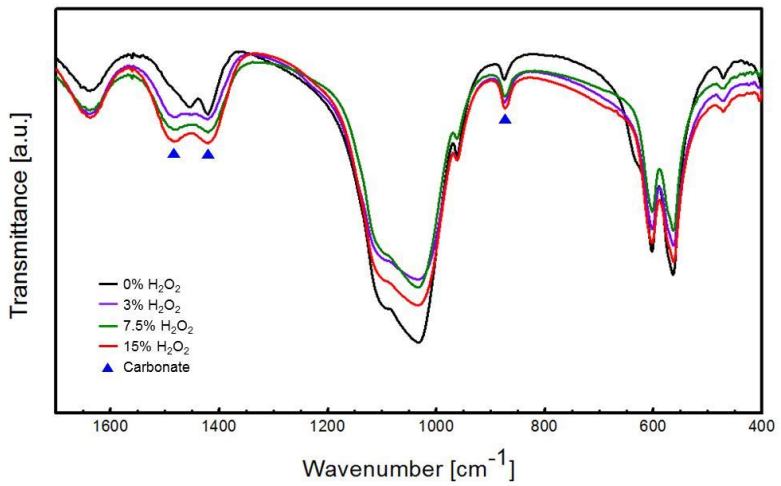

Figure 3.14 Fourier transform infrared (FT-IR) spectra of CHA with different added amount of H_2O_2. As the more H_2O_2 was added to $Ca(OH)_2$ solution, more carbonate was substituted into the CHA structure.

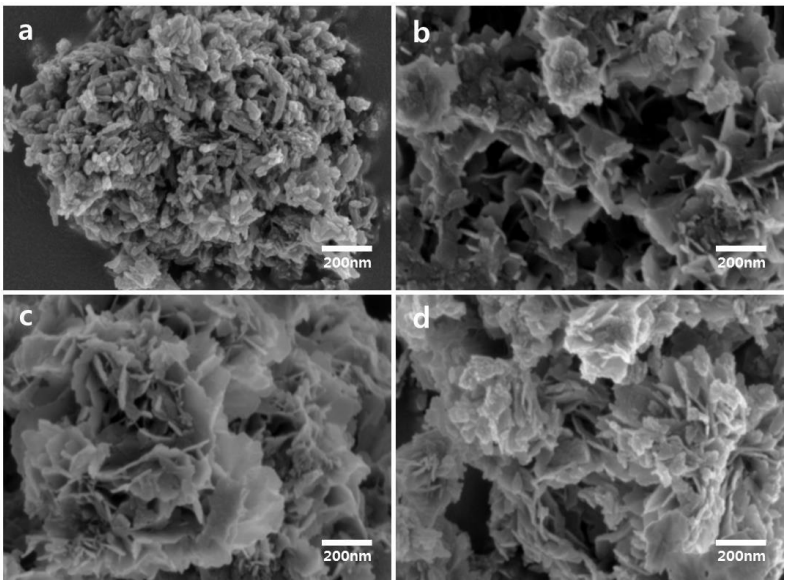

Figure 3.15 FESEM images of synthesized CHA particles with different added amount of H_2O_2 solution. As the more H_2O_2 was added to $Ca(OH)_2$ solution, rice shape particles were disappeared and flower shape particles were formed. **a,** 0% H_2O_2 (HAP). **b,** 3% H_2O_2. **c,** 7.5% H_2O_2. **d,** 15% H_2O_2.

Chapter 4. CONCLUSION

In this research, we synthesized nano-carbonate hydroxyapatite using the wet precipitation. Compared to the previous reported carbonate hydroxyapatite synthesis, we use atmospheric CO_2 as carbon source for CO_3 groups in carbonate hydroxyapatite instead of using carbon containing chemicals. To accelerate CO_2 absorption efficiency, we used H_2O_2 solution during the synthesis. After that, CHA precipitation was conducted by adding H_3PO_4 solution to the $Ca(OH)_2$ and H_2O_2 blending suspension.

For the confirmation of the carbonate hydroxyapatite formation, we conducted comparison study between hydroxyapatite and synthesized carbonate hydroxyapatite using XRD and FESEM. The XRD result showed that the peaks of carbonate hydroxyapatite were shifted to higher angle compared to hydroxyapatite because of CO_3 substitution. FESEM image showed that the morphology of carbonate hydroxyapatite particle was flower shape while the shape of hydroxyapatite particle was rice. In addition, the FT-IR spectrum of synthesized carbonate hydroxyapatite showed that the CO_3 was substituted in the carbonate hydroxyapatite structure.

To prove our insist that the carbon source of CO_3 in carbonate hydroxyapatite was originated from the atmospheric CO_2, we carried out gas chromatography experiment. The result showed that the actual CO_2 absorption

was occur, and $Ca(OH)_2$ and H_2O_2 mixed suspension absorbed CO_2 efficiently. Moreover, we confirmed that superoxide anion radical was generated in the $Ca(OH)_2$ and H_2O_2 blending through the EPR analysis. This demonstrated that superoxide anion radical, the strong nucleophile, was involved in the CO_2 capturing process which occurred during the carbonate hydroxyapatite synthesis.

We also figure out that H_2O_2 affect substituted amount of CO_3 and particle morphology. The higher H_2O_2 concentration of suspension induced more CO_3 substitution in carbonate hydroxyapatite structure. This result showed that H_2O_2 played a huge role in CO_2 mineralization. As more H_2O_2 was used in the carbonate hydroxyapatite synthesis, more particles had flower shape. The element analyzer demonstrated that large amount of CO_2 was absorbed in particle synthesis system, and CHA synthesized with H_2O_2 had similar chemical composition to natural bone.

In conclusion, we successfully synthesized carbonate containing hydroxyapatite using CO_2 capture and wet precipitation method. In addition, we controlled the substituted amount of CO_3 in carbonate hydroxyapatite by changing amount of H_2O_2. The synthesized carbonate hydroxyapatite had similar chemical composition of natural bone. Therefore, our synthesis method can contribute to CO_2 removing, and synthesized carbonate hydroxyapatite can be used as bone graft material.

References

1 Driessens F. C. M. & Verbeeck R. M. H. *Biominerals* (CRC Press INC, 1990).

2 Kaylene J. Q. Melick R. A. Patricia J. B. & Susan M. M. Chemical composition of human bone. *Archs oral biol* **28**, 665-674 (1983)

3 Young M.F. Bone matrix proteins: their function, regulation, and relationship to osteoporosis. *Osteoporos Int* **14**, S35–S42 (2003)

4 Iain R. G. & William B. Novel synthesis and characterization of an AB-type carbonate-substituted hydroxyapatite. J Biomed Mater Res 59, 697-708 (2002)

5 Elia B. Biominerals –hierarchical nanocomposites: the example of bone. *Wiley Interdiscip Rev Nanomed Nanobiotechnol* **3**, 47-69 (2011)

6 Colfen H. Biomineralization: A crystal-clear view. *Nature Materials* **9**, 960-961 (2010)

7 Fergal J. O. Biomaterials & scaffolds for tissue engineering. *Materials today* **14**, 88-95 (2011)

8 Mirjam F. Warren L. G. Leo G. W. *et al*. Tissue engineering bone grafts: biological requirements, tissue culture and clinical relevance. *Curr Stem Cell Res Ther* **3**, 254-264 (2008)

9 Eng S. T. Zeeshan A. Jie H. *et al*. The role of electrosprayed apatite nanocrystals in guiding osteoblast behavior. *Biomaterials* **29**, 1833-1843 (2008)

10 Despina D. D. Mikoleta D. K. Petros G. K. & Yiannis F. M. Effect of

surface roughness of hydroxyapatite on human bone marrow cell adhesion, proliferation, differentiation and detachment strength. *Biomaterials* **22**, 87-96 (2000)

11 Hajime O. Yoshiko D. Susumu T. & Shiro T. Osteogenic differentiation of marrow stromal stem cells in porous hydroxyapatite ceramics. *J biomed mater res A* **27**, 1401-1407 (1993)

12 Noriyuki T. Akira M. Tetsuya T. et al. Novel hydroxyapatite ceramics with an interconnective porous structure exhibit superior osteoconduction in vivo, *J biomed mater res A* **59**, 110-117 (2002)

13 K. Rezwan, Q.Z. Chen, J. J. Blaker, & Aldo R. B. Biodegradable and bioactive porous polymer/inorganic composite scaffods for bone tissue engineering. *Biomaterials* **27**, 3413-3431 (2006)

14 Akira O. Tetsuo H. Hiroyuki K. et al. Comparison of hydroxyapatite and beta tricalcium phosphate as bone substitutes after excision of bone tumors. *J biomed mater res B* **72**, 94-101 (2005)

15 Hibi A. Ishikawa T. Asano M. et al. A study of failed implantation of hydroxyapatite for benign bone tumor. *Orthoped surg* **45**, 1423-1428 (1994)

16 K. de Groot. Bioceramics consisting of calcium phosphate salts. *Biomaterials* **1**, 47-50 (1980)

17 Michael J. Calcium phosphate ceramics as hard tissue prosthetics. *Clin orthop* **157**, 259-278 (1981)

18 Kazuhisa S. & Vert M. Comparative study of porous hydroxyapatite and tricalcium phosphate as bone substitute. *J orthop res* **3**, 301-310 (1985)

19 Takatoshi O. Koji I. Ikuho Y. at el. The effect of the microstructure of β-

tricalcium phosphate on the metabolism of subsequently formed bone tissue. *Biomaterials* **28**, 2612-2621 (2007)

20 R. Ramachandra R, H. N. Roopa, T. S. Kannan. Solid state synthesis and thermal stability of HAP and HAP- βTCP composite ceramic powders. *J mater sci mater med* **8**, 511-518 (1997)

21 Anik P. Erna A. P. D. Christian V. A. & Ronald M. H. V. Solid modeled by ab initio crystal-field methods. 12. Structure, orientation, and position of A-type carbonate in a hydroxyapatite lattice. *J phys chem B* **101**, 3995-3998 (1997)

22 Wallaeys R. Study of carbonate apatite obtained by solid state synthesis. In: silicon, Sulphur, phosphates. *Coll in union pure appl chem munster. Weinheim: verlag chemi,* 183-190 (1954)

23 Elliott J. C. On the interpretation of the carbonate bands in the infrared spectrum of dental enamel. *J dent res* **42**, 1081 (1963)

24 Ito A. Maekawa K. Tsutsumi S. at el. Solubility product of OH-carbonated hydroxyapatite. *J biomed mater res* **36**, 522-528 (1997)

25 Nordstrom E. G. Karlsson K. H. Carbonate-doped hydroxyapatite. *J mater sci mater med* **1**, 182-184 (1990)

26 Nelson D. G. A. & Featherston J. D. B. Preparation, analysis and characterization of carbonated apatites. *Calcif tissue int* **34**, S69-81 (1982)

27 Vignoles M. Bonel G. & Young R. A. Occurrence of nitrogenous species in precipitated B-type carbonated hydroxyapatite. *Calcif tissue int* **40**, 64-70 (1987)

28 Vignoles M. Bonel G. Holcomb D. W. & Young R. A. Influence of

preparation conditions on the composition of type-B carbonated hydroxyapatite and on the localization of the carbonate ions. *Calcif tissue int* **43**, 33-40 (1988)

29 Doi Y. Moriwaki Y. Okazaki M. et al. Carbonate apatites from aqueous and nonaqueous media studied by E.S.R., I.R. and X-ray diffraction: effect of NH_4^+ ions on crystallographic parameters. *J dent Res* **61**, 429-434 (1982)

30 Rey C. Collins B. Goehl T. et al. The carbonate environment in bone mineral: A resolution-enhanced fourier transform infrared spectroscopic study. *Calcif tissue int* **45**, 157-164 (1989)

31 Haobo P. & Brian W. D. Effect of carbonate on hydroxyapatite solubility. *Cryst growth des* **10**, 845-850 (2010)

32 R. Z. Le geros. Calcium phosphates in oral geology and medicine. Monographs in oral science, AG publishers, 82-107, Basel (1991)

33 A. Porter, N. Partel, R. Brooks. et al. Effect of carbonate substitution on the ultrastructural characteristics of hydroxyapatite implants. *J mater sci mater med* **16**, 899-907 (2005)

34 Asha R. Lilia A. H. Frank R. et al. osteoblast activity on carbonate hydroxyapatite. *J biomed mater res A* **100**, 1089-1096 (2012)

35 Gavin S. Nelesh P. Roger B. & Neil R. Carbonate substituted hydroxyapatite: resorption by osteoclasts modifies the osteoblastic response. *J biomed mater res A* **90**, 217-224 (2009)

36 Keiichi K. Wantida S. Hitoyata S. et al. Osteoclast and osteoblast activities on carbonate apatite plates in cell cultures. *J biomater appl* **26**, 435-449 (2011)

37 E. Landi, G. Celotti, G. Logroscino, & A. Tampieri. Carbonated hydroxyapatite as bone substitute. *J eur ceram soc* **23**, 2931-2937 (2003)

38 Cai S. Wang . Lv H. et al. Synthesis of carbonate hydroxyapatite nanofibers by mechanochemical methods. *Ceram int* **31**, 135-138 (2005)

39 J.C. Merry, I. R. Gibson, S.M. Best, & W. Bonfield. Synthesis and characterization of carbonate hydroxyapatite. *J mater sci mater med* **9**, 779-783 (1998)

40 A.H. Rajabi-Zamani, A. Behnamghader, & A. Kazemzadeh. Synthesis of nanocrystalline carbonated hydroxyapatite powder via nonalkoxide sol-gel method. *Mater sci eng C* **28**, 1326-1329 (2008)

41 Renato B. Giuseppe S. & Marco M. Process design and energy requirements for the capture of carbon dioxide from air. *Chem eng process* **42**, 1047-1058 (2006)

42 Cheng-Hsiu Y. Chih-Hung H. & Chung-Sung T. A review of CO_2 capture by absorption and adsorption. *Aerosol and air quality research* **12**, 745-769 (2012)

43 IPCC. Special report on carbon dioxide capture and storage. *Intergovermental panel on Climate Change* (Cambridge University Press, 2005)

44 John A. Turner. A realizable renewable energy future. *Science* **30**, 687-689 (1999)

45 Earth science communications team at NASA's jet propulsion laboratory/California institute of technology. Global climate change. (NOAA)

46 Jon G. & Hannah C. Carbon capture and storage. *Energy policy* **36**,

4317-4322 (2008)

47 Soren A. & Richard N. Prospects for carbon capture and storage technologies. *Annu rev environ resour* **29**, 109-142 (2004)

48 Stuart H. How to bury the problem. *Chemistry world Oct*, 42-46 (2007)

49 K. Michael, A. Golab, V. Shulakova, et al. Geological storage of CO_2 in saline aquifers-a review of the experience from existing storage operations. *Int J greenhouse gas control* **4**, 659-667 (2010)

50 J. Hansen, M. Sato, P. Kharecha, et al. Target atmospheric CO_2: where should humanity aim?. *Open Atmos Sci J* **2**, 217-231 (2008)

51 Elliott S. Lackner K. S., Ziock H. J. et al. Compensation of atmospheric CO_2 build up through engineered chemical sinkage. *Geophysical research letters* **28**, 1235-1238 (2001)

52 Lackner K. S. Sarah B. Jurg M. M. et al. The urgency of the development of CO_2 capture from ambient air. *PNAS* **109**, 13156-13162 (2012)

53 Lackner K. S. Capture of carbon dioxide from ambient air. *Eur phys J special topics* **176**, 93-106 (2009)

54 Lackner K. S. Grimes P. Ziock H-J. et al. Carbon dioxide extraction from air: is it option?. *Technical report LA-UR-99-583* (Los Alamos National laboratory, Los Alamos, NM, 1999)

55 Keith D. Ha-Duong M. & Stolaroff J. K. Climate stratagy with CO_2 capture from the air. *Climatic change* **74**, 17-45 (2006)

56 Zeman F. S. & Lackner K. S. Captureing carbon dioxide directly from the atmosphere. *World resources review* **16**, 62-68 (2004)

57 Dubey M. Ziock H. Rueff G. et al. Extraction of carbon dioxide from

the atmosphere through engineered chemical sinkage. *ACS-division of fuel chemistry reprints* **47**, 81-84 (2002)

58 Nikulshina V. Galvez M. E. & Steinfeld A. Kinetic analysis of the carbonation reactions for the capture of CO_2 from air via the Ca(OH)2-$CaCO_3$-CaO solar thermochemical cycle. *Chem eng J* **129**, 75-83 (2007)

59 Joshual K. S. David W. K. & Gregory V. L. Carbon dioxide capture from atmospheric air using sodium hydroxide spray. *Envion sci technol* **42**, 2728-2735 (2008)

60 Sang-Jun H. Dae-Kyeong K. Jae-Hee L. et al. Capture of carbon dioxide emitted from coal-fired power plant using seawater. *J Kor soc environ eng* **35**, 340-349 (2013)

61 Nathan J. Dwight M. Elizabeth O. & Evan C. Interactions of water vapor with oxides at elevated temperatures. *J phys chem solids* **66**, 471-478 (2005)

62 Rajan R. V. Jih-Gaw L. & Bill T. R. Low-level chemical pretreatment for enhanced sludge solubilization. *Res J water pollut cont Feder* **61**, 1678-1683 (1989)

63 Bei W. Yanqun L. Nan W. & Christopher Q. L. CO_2 bio-mitigation using microalgae. *Appl microbio biotech* **79**, 707-718 (2008)

64 Thamilselvan S. Byer K. J. Hackett R. L. & Khan S. R. Free radical scavengers, catalase and superoxide dismutase provide protection from oxalate-associated injury to LLC-PK1 and MDCK cells. *J Urol* **164**, 224-229 (2000)

65 Yong M. Bo-Tao Z. Lixia Z. et al. Study on the generation mechanism of reactive oxygen species on calcium peroxide by chemiluminescence

and UV-visible spectra. *Luminescence* **22**, 575-580 (2007)

66 Tsentsiper A. B. & Vasil'eva R. P. The reaction of calcium hydroxide with hydrogen peroxide vapor. 2445-2447 (*UDC 546.41+54-36+546.215*)

67 Ballou E. V. Wood P. C. & Spitze L. A. The preparation of calcium superoxide from calcium peroxide deperoxyhydrate. *Ind eng chem prod res dev* **16**, 180-186 (1977)

68 Sang-Jun H. Miran Y. Dong-Woo K. & Jung-Ho W. Carbon dioxide capture using calcium hydroxide aqueous solution as the absorbent. *Energy & fuels* **25**, 3825-3834 (2011)

69 Uri S. Zach B. & Yoel S. New technology for post-combustion abatement of carbon dioxide *via* an *in situ* generated superoxide anion-radical. *RSC adv* **4**, 36544-36552 (2014)

70 Akane S. Kana T. Takeo T. et al. Target-selective degradation of proteins by a light-activated 2-phenylquinoline-estradiol hybrid. *Chem commun* **41**, 4260-4262 (2007)

71 R.N. Panda, M.F. Hsieh, R. J. Chung, & T. S. Chin. FTIR, XRD, SEM and solid state NMR investigations of carbonate-containing hydroxyapatite nano-particles synthesized by hydroxide-gel technique. *J phys chem solids* **64**, 193-199 (2003)

72 E. Landi, G. Celotti, G. Logroscino, & A. Tampieri. Carbonate hydroxyapatite as bone substitute. *J eur ceram soc* **23**, 2931-2937 (2003)

73 Yuhui S. Wai C. C. L. Chunyi W. & Wenhai H. Bone regeneration: Importance of lacal pH – strontium-doped borosilicate scaffold. *J mater chem* **22**, 8662-8670 (2012)

74 A. B. Tsentisiper & R. P. Vasil'eva. The reaction of calcium hydroxide with hydrogen peroxide vapor. *Russ Chem Bull* **16**, 2445-2447 (1967)

75 Cheng-Hsiu Y. Chih-Hung H. & Chung-Sung T. A review of CO_2 capture by absorption and adsorption. *Aerosol and air quality research* **12**, 745-769 (2012)

초 록

최근, 뼈와 관련하여 발생하는 질병이나 부상을 치료하기 위하여 칼슘 포스페이트 계열의 물질들이 뼈 임플란트로 많이 사용되고 있다. 현재 가장 많이 사용되는 재료는 하이드록시 아파타이트와 트리칼슘 포스페이트로 뼈의 주성분인 칼슘과 포스페이트로 이루어진 칼슘 포스페이트 계열의 화합물이다. 하지만 실제 뼈는 칼슘과 포스페이트 외에도 탄산이나 나트륨, 칼륨과 같은 다른 성분들을 가지고 있기 때문에 많은 연구들이 칼슘과 포스페이트 이외의 이온을 하이드록시 아파타이트 내부에 치환시켜 뼈와 비슷한 조성의 임플란트 재료를 만들려는 시도를 하고 있다. 탄산은 뼈에 칼슘과 포스페이트 다음으로 많이 존재하는 물질로, 이로인해 탄산기를 포함하고 있는 하이드록시 아파타이트에 대해 많은 관심이 쏠리고 있다. 탄산 하이드록시 아파타이트는 기존의 하이드록시 아파타이트와 같이 높은 생체 적합성을 나타내며, 생체 내 분해성을 가지고 있어서 체내에 이식되었을 때 자연골로 치환될 수 있다는 장점을 지닌다. 이러한 장점을 가진 탄산 하이드록시 아파타이트를 합성하기 위한 많은 방법이 존재하는데, 대부분의 방법들이 탄산의 근원이 되는 탄소를 포함한 화학물질을 첨가하여 합성한다.

본 연구에서는 탄소를 포함한 화학물질을 첨가하는 대신, 슈퍼옥사이드 음이온 라디칼을 합성 시스템 내에 생성, 공기 중의 이산화탄소를 흡수하여 탄산 하이드록시 아파타이트를 균일 침전법을 통해 합성하고자 하였다. 합성된 물질의 특성을 파악하기 위해 X-선 회절법, 흡광 분석을 시행하였으며, 그 결과 성공적으로 탄산 하이드록시 아파타이트가 합성되었음을 확인하였다. 그 다음, 실제로 공기 중의 이산화탄소를 흡수하는지 확인하기 위하여 가스 크로마토그래피 분석을 진행하였다. 그 결과, 실제 우리의 합성

시스템이 많은 양의 이산화탄소를 흡수하는 것을 확인하였고, 흡수 과정에서 슈퍼옥사이트 음이온 라디칼이 관여하는 것을 확인하였다. 이후, 상분석을 통해 이산화탄소의 석화 작용이 일어나 탄산 칼슘이 생성되고, 인산 첨가 후에 중간상인 인산 이칼슘을 지나 마침내 탄산 하이드록시 아파타이트가 생성되는 상변화를 관찰하였다. 마지막으로 합성 시 첨가하는 과산화수소의 양을 조절하여 자연골이 지니는 탄산 량의 범위 내에서 합성된 탄산 하이드록시 아파타이트 내부의 탄산 양을 조절하는데 성공하였으며, 결과적으로 합성된 탄산 하이드록시 아파타이트가 뼈와 비슷한 조성을 나타낸다는 것을 확인하였다.

본 연구는 크게 두 가지 관점에서 의의를 가진다. 첫째, 기존의 탄산을 포함한 화합물을 첨가하는 합성법과 달리 공기 중에 풍부하게 존재하는 이산화탄소를 미네랄라이즈 시켜, 탄산 하이드록시 아파타이트 내부에 존재하는 탄산기의 원료로 사용하는 새로운 방법을 제시하고 있다. 둘째, 합성된 탄산 하이드록시 아파타이트는 뼈와 비슷한 조성을 가지고 있기 때문에 뼈 임플란트 재료로써 사용될 수 있다. 따라서, 기존의 이산화탄소를 흡수, 저장만 했던 시스템을 해결하는 동시에 뼈 임플란트 재료를 합성하는 획기적인 방법을 제시하고 있다.

주요어: 탄산 하이드록시 아파타이트, 균일 침전법, 이산화탄소 흡수, 슈퍼옥사이드 음이온 라디칼, 임플란트 재료, 뼈
학 번: 2014-21458